

## **INFORMATION TO USERS**

While the most advanced technology has been used to photograph and reproduce this manuscript, the quality of the reproduction is heavily dependent upon the quality of the material submitted. For example:

- Manuscript pages may have indistinct print. In such cases, the best available copy has been filmed.
- Manuscripts may not always be complete. In such cases, a note will indicate that it is not possible to obtain missing pages.
- Copyrighted material may have been removed from the manuscript. In such cases, a note will indicate the deletion.

Oversize materials (e.g., maps, drawings, and charts) are photographed by sectioning the original, beginning at the upper left-hand corner and continuing from left to right in equal sections with small overlaps. Each oversize page is also filmed as one exposure and is available, for an additional charge, as a standard 35mm slide or as a 17"x 23" black and white photographic print.

Most photographs reproduce acceptably on positive microfilm or microfiche but lack the clarity on xerographic copies made from the microfilm. For an additional charge, 35mm slides of 6"x 9" black and white photographic prints are available for any photographs or illustrations that cannot be reproduced satisfactorily by xerography.



8703705

**Feiz, Masoud**

DEVELOPMENT OF A POLYNOMIAL NODAL MODEL TO THE MULTIGROUP  
TRANSPORT EQUATION IN ONE DIMENSION

*Iowa State University*

PH.D. 1986

University  
Microfilms  
International

300 N. Zeeb Road, Ann Arbor, MI 48106



Development of a polynomial nodal model to the multigroup  
transport equation in one dimension

by

Masoud Feiz

A Dissertation Submitted to the  
Graduate Faculty in Partial Fulfillment of the  
Requirements for the Degree of  
DOCTOR OF PHILOSOPHY

Major: Nuclear Engineering

Approved:

Signature was redacted for privacy.

In Charge of Major Work

Signature was redacted for privacy.

For the Major Department

Signature was redacted for privacy.

For the Graduate College

Iowa State University  
Ames, Iowa

1986

## TABLE OF CONTENTS

	Page
I. INTRODUCTION	1
II. LITERATURE REVIEW	4
A. Spherical Harmonics Method	5
B. Discrete Ordinates Method	8
C. Finite Element Method	9
D. Nodal Method	11
III. DEVELOPMENT OF THE ONE-DIMENSIONAL MULTIGROUP $P_N$ EQUATIONS	14
IV. APPLICATION OF THE NODAL MODEL TO THE MULTIGROUP $P_N$ EQUATIONS IN ONE DIMENSION	17
A. Development of the Multigroup $P_N$ Equations in One-Dimensional Nodal Geometry	18
B. Theoretical Development for a Full Expansion	19
C. Theoretical Development for a Partial Expansion	22
D. Interface and Boundary Conditions	25
E. Derivation of the Effective Multiplication Factor	29
V. COMPUTER PROGRAM, SAMPLE PROBLEMS, AND RESULTS	32
A. $P_1$ Approximation for a Full and Partial Expansion	32
B. $P_3$ and $P_5$ Approximations for a Full Expansion	41
VI. SUMMARY AND CONCLUSIONS	53
VII. SUGGESTIONS FOR FUTURE RESEARCH	56
VIII. REFERENCES	57
IX. ACKNOWLEDGMENTS	59
X. APPENDIX	60

## LIST OF FIGURES

	Page
Figure III-1. Multigroup partitioning of the energy range	14
Figure IV-1. One-dimensional nodal geometry	18
Figure IV-2. Interface conditions for the nodal geometry	26
Figure V-1. Fuel loading pattern for the one-dimensional model, problem 1	33
Figure V-2. Fast flux profiles for sample problem one	34
Figure V-3. Thermal flux profiles for sample problem one	34
Figure V-4. Magnitude of the relative terms in equation V-1 for sample problem one, using a full expansion	36
Figure V-5. Magnitude of the relative terms in equation V-2 for sample problem one, using a full expansion	36
Figure V-6. Magnitude of the relative terms in equation V-1 for sample problem one, using a partial expansion	38
Figure V-7. Magnitude of the relative terms in equation V-2 for sample problem one, using a partial expansion	38
Figure V-8. Fast current profiles for sample problem one	39
Figure V-9. Thermal current profiles for sample problem one	39
Figure V-10. Fuel loading pattern for the one-dimensional model, problem 2	43
Figure V-11. Thermal flux profiles for sample problem two	44
Figure V-12. Magnitude of the relative terms in equation V-5 for sample problem two	45
Figure V-13. Magnitude of the relative terms in equation V-6 for sample problem two	45
Figure V-14. Magnitude of the relative terms in equation V-7 for sample problem two	46

	Page
Figure V-15. Magnitude of the relative terms in equation V-8 for sample problem two	46
Figure V-16. Magnitude of the relative terms in equation V-9 for sample problem two	47
Figure V-17. Magnitude of the relative terms in equation V-10 for sample problem two	47
Figure V-18. $P_1$ weight of the thermal flux for sample problem two	49
Figure V-19. $P_2$ weight of the thermal flux for sample problem two	49
Figure V-20. $P_3$ weight of the thermal flux for sample problem two	50
Figure V-21. $P_4$ weight of the thermal flux for sample problem two	50
Figure V-22. $P_5$ weight of the thermal flux for sample problem two	51
Figure V-23. Eigenvalue convergence of sample problem two	51

## LIST OF TABLES

	Page
Table V-1. Benchmark fuel parameters	33
Table V-2. Nuclear fuel data	41

## I. INTRODUCTION

The central problem of nuclear reactor theory is the determination of the spatial, energy, and time distribution of neutrons within the reactor. This is due to the fact that the neutron distribution determines the rate at which different nuclear reactions occur inside the reactor. The fundamental equation describing the distribution of neutrons is the neutron transport equation. It is a conservation equation for the neutron distribution as a function of time, position, direction of motion, and neutron energy [1,2]. The transport equation is the basic component in the development of models for nuclear reactor design and fuel management. It is the starting point for the development of the neutron diffusion theory which is adapted to most reactor applications [2].

The neutron diffusion theory is an approximation to the more complicated transport theory and is quite adequate for many calculations and results in considerable simplification over transport theory. However, diffusion theory is in error for cases where the flux gradients become very large. Such cases are found to be at interfaces between dissimilar regions, and near the surfaces of strong neutron absorbers or localized sources [2]. In such cases, the transport theory should be adapted to analyze the behavior of the neutrons.

Different schemes have been developed for analyzing the neutron transport equation [1]. Spherical harmonics, Fourier transform, discrete ordinates, Monte Carlo, and finite element methods are typical

techniques that are used in finding an approximate solution to the transport equation. The spherical harmonics method forms the theoretical basis for diffusion theory, and the Fourier transform method justifies the few-group approximation [1]. The discrete ordinates, Monte Carlo, and finite element methods are the most commonly used schemes in analyzing reactor problems in which a detailed accounting of the transport theory effects is important.

Discrete ordinates and finite element methods are direct numerical solutions to the neutron transport equation, and when applied, a suitable algorithm for solving the resulting equations should then be developed. One of the disadvantages of using the discrete ordinates method arises when the geometry of the reactor becomes complex. In that case, a large number of spatial and angular mesh points are required which, in turn, would make the discrete ordinates approach time consuming and very expensive [3]. The finite element method, on the other hand, is more efficient than the discrete ordinates method in the sense that fewer spatial and angular mesh points are usually needed to describe the complex geometry [1].

A technique that has been quite successful in providing relatively low-cost calculations of three-dimensional power distributions, using the diffusion theory approximation, is the nodal method. The nodal method is based upon dividing the reactor into a number of large volumetric regions called nodes [2]. The average flux and the outgoing currents at each surface of the nodal volume are assumed to be functions of the properties within the volume and the current entering each

node. Unfortunately, the nodal method has not been applied to the neutron transport equation to any great extent.

It is the purpose of this study to develop and test a nodal model that can be used to solve the one-dimensional multigroup form of the neutron transport equation. Earlier studies of the one-dimensional diffusion equation, using the nodal model, have proven to be successful [4,5].

## II. LITERATURE REVIEW

The neutron distribution in a nuclear reactor can be found by solving the neutron transport equation. The transport equation is often called the Boltzmann equation due to the fact that it is similar to the equation obtained by L. Boltzmann in connection with the kinetic theory of dilute gases [3,6]. The steady state neutron transport equation is given by the following integro-differential equation [1]:

$$\begin{aligned} \underline{\Omega} \cdot \nabla \psi(\underline{r}, \underline{\Omega}, E) + \Sigma_t(\underline{r}, E) \psi(\underline{r}, \underline{\Omega}, E) = \\ \int dE' \int d\underline{\Omega}' \left[ \sum_j \frac{1}{\lambda} \chi^j(E) v^j \Sigma_f^j(\underline{r}, E') + \right. \\ \left. \Sigma_s(\underline{r}, \underline{\Omega}' \rightarrow \underline{\Omega}, E' \rightarrow E) \right] \psi(\underline{r}, \underline{\Omega}', E') + Q(\underline{r}, \underline{\Omega}, E) \end{aligned} \quad (\text{II-1})$$

where:

$\underline{\Omega}$  = Angular direction.

$\psi(\underline{r}, \underline{\Omega}, E)$  = Angular neutron flux.

$\Sigma_t(\underline{r}, E)$  = Total macroscopic interaction cross section  
by absorption and scattering.

$\lambda$  = The effective multiplication factor.

$v^j \Sigma_f^j(\underline{r}, E')$  = Macroscopic cross section for neutron production  
due to fission at energy  $E'$  for isotope  $j$ .

$\chi^j(E)$  = Fission spectrum of isotope  $j$ .

$\Sigma_s(\underline{r}, \underline{\Omega}' \rightarrow \underline{\Omega}, E' \rightarrow E)$  = Differential scattering cross section from  $E'$  and  
direction  $\underline{\Omega}'$  into the interval  $dE d\underline{\Omega}$ .

$Q(\underline{r}, \underline{\Omega}, E)$  = Extraneous (i.e., nonfission) source density.

The angular neutron density in the one-dimensional geometry depends only on  $Z$  and  $\mu$ , where  $\mu$  is the dot product of  $\underline{\Omega}$  with a unit vector specifying the direction of the  $Z$  axis. Therefore, the neutron transport equation in one dimension becomes [1]:

$$\begin{aligned} \mu \frac{\partial}{\partial Z} \psi(Z, \mu, E) + \Sigma_t(Z, E) \psi(Z, \mu, E) = \\ \int_0^\infty dE' \int_{-1}^{+1} \frac{d\mu'}{2} \sum_j \frac{1}{\lambda} \chi^j(E) v^j \Sigma_f^j(Z, E') \psi(Z, \mu', E') + \\ \int_0^\infty dE' \int_{-1}^{+1} \frac{d\mu'}{2} \Sigma_s(Z, E' \rightarrow E, \mu_0) \psi(Z, \mu', E') \end{aligned} \quad (\text{II-2})$$

where the differential scattering cross section is assumed to depend only on  $\mu_0$  ( $\mu_0 = \underline{\Omega} \cdot \underline{\Omega}'$ ), the cosine of the scattering angle. The extraneous source has also been dropped from equation II-2.

Of the different schemes that have been developed for approximating a solution to the transport equation [1], the following methods will be considered:

- A. Spherical Harmonics Method.
- B. Discrete Ordinates Method.
- C. Finite Element Method.
- D. Nodal Method.

A brief discussion of each follows.

#### A. Spherical Harmonics Method [1,3,7]

The spherical harmonics method is one of the most commonly used schemes for solving the one-dimensional neutron transport equation.

The essential basis of this method is that the angular dependence of the neutron flux is expanded in a complete set of elementary functions, such as a series of polynomials.

The spherical harmonics method is formulated for the one-dimensional form of the transport equation. In this case, the spherical harmonics reduces to the Legendre polynomials with coefficients that are functions of  $Z$  and  $E$ . Therefore, the angular neutron flux and the differential scattering cross section in equation II-2 could be expanded in a series of Legendre polynomials as:

$$\psi(Z, \mu, E) = \sum_{n=0}^{\infty} (2n+1) \psi_n(Z, E) P_n(\mu) \quad (\text{II-3})$$

$$\Sigma_s(Z, E' \rightarrow E, \mu_0) = \sum_{n=0}^{\infty} (2n+1) \Sigma_{sn}(Z, E' \rightarrow E) P_n(\mu_0) \quad (\text{II-4})$$

where:

$$\Sigma_{sn}(Z, E' \rightarrow E) = \int_{-1}^{+1} \frac{d\mu_0}{2} \Sigma_s(Z, E' \rightarrow E, \mu_0) P_n(\mu_0) \quad (\text{II-5})$$

The  $P_n(\mu)$  functions are the Legendre polynomials (see the Appendix), and  $\psi_n(Z, E)$  are the expansion coefficients.

The expansions in equations II-3 and II-4 are now substituted into the one-dimensional neutron transport equation (II-2):

$$\begin{aligned} & \sum_{n=0}^{\infty} \left\{ (2n+1) \mu P_n(\mu) \frac{\partial}{\partial Z} \psi_n(Z, E) + \Sigma_t(Z, E) (2n+1) P_n(\mu) \psi_n(Z, E) \right\} = \\ & \int_0^{\infty} dE' \int_{-1}^{+1} \frac{d\mu'}{2} \left[ \sum_j \frac{1}{\lambda} \chi^j(E) \nu^j \Sigma_f^j(Z, E') \right] \left[ \sum_{n=0}^{\infty} (2n+1) P_n(\mu') \psi_n(Z, E') \right] + \\ & \int_0^{\infty} dE' \int_{-1}^{+1} \frac{d\mu'}{2} \left[ \sum_{n=0}^{\infty} (2n+1) \Sigma_{sn}(Z, E' \rightarrow E) P_n(\mu_0) \right] \left[ \sum_{m=0}^{\infty} (2m+1) P_m(\mu') \psi_m(E') \right] \end{aligned} \quad (\text{II-6})$$

The recurrence relation (see the Appendix) is then used in the first term on the left of equation II-6, and the law of angular addition of Legendre polynomials is used to express  $P_n(\mu_0)$  in terms of  $P_n(\mu')$  and  $P_n(\mu)$ . The resulting expression is then multiplied by  $(2n+1)P_n(\mu)$  and integrated over  $\mu$  from  $(-1)$  to  $(+1)$ . Upon using the orthogonality of the Legendre polynomials, one has

$$\begin{aligned}
 & n \frac{\partial}{\partial Z} \psi_{n-1}(Z, E) + (n+1) \frac{\partial}{\partial Z} \psi_{n+1}(Z, E) + (2n+1) \Sigma_t(Z, E) \\
 \psi_n(Z, E) = & \delta_{0n} \int_0^\infty dE' \sum_j \frac{1}{\lambda} \chi^j(E) v^j \Sigma_f^j(Z, E') \psi_0(Z, E') + \\
 & (2n+1) \int_0^\infty dE' \Sigma_{sn}(Z, E' \rightarrow E) \psi_n(Z, E') \quad (\text{II-7})
 \end{aligned}$$

where  $\delta_{0n}$  is the Kroneker delta, i.e.,

$$\delta_{0n} = 1 \quad \text{if } n = 0 \quad \text{and} \quad \delta_{0n} = 0 \quad \text{if } n \neq 0$$

The neutron transport equation is then replaced by a system of  $(N+1)$  coupled differential equations in the moments of the angular neutron flux. The  $P_N$  approximation results when the derivative of the  $(N+1)$ th moment and higher moments of the angular neutron flux are neglected.

The incentive in using the Legendre polynomial expansion of the angular neutron flux is that the first two terms have a simple physical meaning. For  $n=0$ , the scalar neutron flux density is given by  $\psi_0(Z)$ , and for  $n=1$ , the neutron current density is given by  $\psi_1(Z)$ , or  $J(Z)$ . Note that  $N=1$  gives the  $P_1$  approximation which is the diffusion theory approximation.

## B. Discrete Ordinates Method [1,3]

In order to illustrate the discrete ordinates method with a minimum of algebraic complication, the monoenergetic transport equation in plane geometry with isotropic scattering is considered and can be obtained from equation II-2.

$$\begin{aligned} \mu \frac{\partial}{\partial Z} \psi(Z, \mu) + \Sigma_t(Z) \psi(Z, \mu) = \\ \left[ \sum_j \frac{1}{\lambda} \chi^j \nu^j \Sigma_f^j(Z) + \Sigma_s(Z) \right] \int_{-1}^{+1} \psi(Z, \mu') \frac{d\mu'}{2} \end{aligned} \quad (\text{II-8})$$

The general principle of this method is that the angular distribution of the neutron flux is evaluated in a number of specific discrete directions. If equation II-8 is considered for a set of discrete directions ( $\mu_\ell$ ), a set of coupled first order differential equations for  $\psi(Z, \mu_\ell)$  would be obtained. The integral in equation II-8 is then approximated by a numerical quadrature formula involving  $\psi(Z, \mu_\ell)$ , and is represented by:

$$\int_{-1}^{+1} \psi(Z, \mu') \frac{d\mu'}{2} \approx \frac{1}{2} \sum_{\ell=1}^N w_\ell \psi(Z, \mu_\ell) \quad (\text{II-9})$$

where the  $w_\ell$  are the quadrature weights. Using the approximation in II-9, equation II-8 becomes:

$$\begin{aligned} \mu_d \frac{\partial}{\partial Z} \psi(Z, \mu_d) + \Sigma_t(Z) \psi(Z, \mu_d) = \\ \frac{1}{2} \left[ \sum_j \frac{1}{\lambda} \chi^j \nu^j \Sigma_f^j(Z) + \Sigma_s(Z) \right] \sum_{\ell=1}^N w_\ell \psi(Z, \mu_\ell) \\ (d=1, 2, \dots, N) \end{aligned} \quad (\text{II-10})$$

where the set of  $N$  coupled differential equations in space can be solved readily by finite difference techniques. The difference equations are then solved by using an iterative scheme.

The discrete ordinates method is a useful technique for analyzing reactor problems in which the diffusion theory approximation is inadequate [1]. However, the method becomes impractical for two- and three-dimensional geometries since the number of discrete points required to represent the reactor is often very large [8].

### C. Finite Element Method [9-13]

The polynomial representation of the angular neutron flux within a subregion of a core has been considered as an alternative to the discrete ordinates solution of the neutron transport equation. The primary attractions of this method are: the accuracy by which the angular neutron flux is determined using few mesh points; and the fact that the angular neutron flux is found over the whole element, not just at certain mesh points as in the discrete ordinates method [8].

In the finite element method, difference equations are generated by using approximate methods with the piecewise polynomial solution. The unknown coefficients in the expansion functions are found using the weighted residual method. The weighted residual method used in this study is the least squares technique. The least squares technique is formulated for the following problem:

$$L[\psi] = f(U) \tag{II-11}$$

where  $L[\psi]$  is the differential operator involving the spatial derivative of  $\psi$ . The dependent variable  $U$  is assumed to represent a one-dimensional coordinate, although the definition of  $U$  may be interpreted as a coordinate in the multidimensional space. The solution of equation II-11 is often attempted by assuming an approximation to the solution  $\psi(U)$ , an expression in the following form:

$$\psi(U) \approx W(U, a_1, a_2, \dots, a_I) \quad (\text{II-12})$$

where  $I$  denotes the number of coefficients, and the parameters  $a_1$  through  $a_I$  are arbitrary and should be determined such that  $\psi(U)$ , and  $W(U, \underline{a})$  are close in some sense. The function  $W(U, \underline{a})$  may be assumed in the following form:

$$W(U, \underline{a}) = \sum_{i=1}^I a_i T_i(U) \quad (\text{II-13})$$

where the functions  $T_i(U)$  are arbitrary and are called the trial functions.

Substituting equation II-12 into equation II-11, one gets the residual  $R$  since  $W(U, \underline{a})$  is not the exact solution. The residual  $R$  which is a function of  $U$  and  $\underline{a}$  has the following form:

$$R[U, \underline{a}] = L[W(U, \underline{a})] - f(U) \quad (\text{II-14})$$

The  $a_i$ 's are chosen to minimize the integral of the square of the residual  $R$ :

$$L = \int R^2(U, \underline{a}) \frac{dU}{2} = \text{minimum} \quad (\text{II-15})$$

The necessary conditions for L to be minimum are given by

$$\frac{\partial L}{\partial a_i} = \int R(U, \underline{a}) \frac{\partial}{\partial a_i} R(U, \underline{a}) dU = 0 \quad (\text{II-16})$$

(i=1, 2, ..., I)

where i denotes the coefficients.

#### D. Nodal Method

The nodal method is another scheme that is recently being considered to approximate the solution of the neutron transport equation [14]. The nodal method was described by Graves [15]:

In nodal analysis of nuclear-reactor power distribution and neutron multiplication, the reactor is subdivided into an array of nodal volumes, usually equal volumes. Each nodal volume is represented by a set of space-and-energy-averaged neutronics parameters that describe its neutron multiplication and transport properties. Neutron interchange between nodes in a nodal calculation is treated with an array of coupling coefficients in each neutron energy group. Each coupling coefficient represents the probability that a neutron produced at the source node will be removed at a nearby "sink" node. The distribution of neutron source level among the nodes and the system multiplication are obtained by writing a neutron balance equation for each node and solving this system of nodal equations.

The importance of using nodal models in reactor analysis was well-stated by Askew in the summary of a recent international meeting on nodal methods [16].

Coarse mesh methods have demonstrated to be a reliable and useful tool for both reactor designers and operators in predicting the assembly to assembly variations of rating for operating reactors. The most advanced models appear to be capable of doing this with a RMS error of the order of +2%. There is a scope for further refinement in

the modeling of reflectors and shrouds, and in the representation of variations of burnup within an assembly, especially at the core edge or following shuffling of edge assemblies. With improvements of this kind, the models will be capable, given good nuclear data and lattice calculations, of a predictive accuracy of the same order as that of the measurements.

Similar comments were made by Wagner in the summary of an earlier conference on static reactor calculations [17].

With the reactors becoming even larger and requirements for safety and economy getting more stringent, it is generally felt that improved and more consistent mathematical models are needed, that rely on empirical fitting. . . . The primary quantities obtained from coarse mesh nodal solutions are node average fluxes and power. Though average reaction rates are also the primary quantities needed for reactivity balances and depletion calculations, the fact that spatial detail within nodes is lost, is certainly a serious drawback of the conventional nodal method.

Recent developments in the field of nodal reactor analysis methods have shown great promise as stated by Wagner and Koebke [14].

Not very long ago coarse mesh methods were considered as a substitute for the more accurate and more detailed fine-mesh finite-difference methods. The understanding was that the computationally cheap nodal methods implied that compromises had to be made with regard to accuracy and spatial resolution. The recent developments in the area of nodal reactor analysis methods are rapidly changing this picture.

To date, the discrete ordinates and the finite element methods are the schemes that are mostly relied upon to provide detailed solutions of the transport equation. However, these methods become expensive and time consuming as the geometry of the problem becomes complex. The nodal method, on the other hand, does not suffer from these problems.

The nodal model that will be developed in this study is based upon polynomial expansion of the flux in the multigroup form of the  $P_N$  equations. Since the polynomial expansion is not the exact solution, a residual is defined for each neutron group and minimized using the least squares technique of the finite element method.

### III. DEVELOPMENT OF THE ONE-DIMENSIONAL MULTIGROUP $P_N$ EQUATIONS

Since the nodal model is to be applied to the multigroup form of the  $P_N$  equations, the present chapter is devoted to the development of the multigroup theory. The first step in the derivation of the multigroup  $P_N$  equations is to partition the energy range of interest from  $E_{\min}$  to  $E_{\max}$  into a large number,  $G$ , of subintervals  $\Delta E_g$  [1,3]. These subintervals are called energy groups and are labeled in increasing order from high to low energies as in Figure III-1.

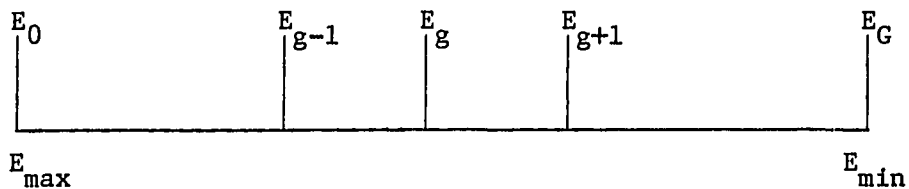


Figure III-1. Multigroup partitioning of the energy range

Therefore,

$$\Delta E_g = E_{g-1} - E_g \quad (g=1,2, \dots, G) \quad (\text{III-1})$$

The next step is to integrate the energy dependent  $P_N$  equations (II-7) over the energy group  $\Delta E_g$ , replacing the integrals on the right by a finite sum of integrals over all the energy groups. In doing so, the result is found to be:

$$\begin{aligned}
& n \frac{d}{dZ} \psi_{n-1}^g(Z) + (n+1) \frac{d}{dZ} \psi_{n+1}^g(Z) + \\
& (2n+1) \Sigma_t^g(Z) \psi_n^g(Z) = \delta_{0n} \sum_{h=1}^G \frac{1}{\lambda} \chi^g \nu \Sigma_f^h(Z) \psi_0^h(Z) + \\
& (2n+1) \sum_{h=1}^G \Sigma_{sn}^{gh}(Z) \psi_n^h(Z) \tag{III-2}
\end{aligned}$$

$(n=0,1, \dots, N)$   
 $(g=1,2, \dots, G)$

In equation III-2, only one fissionable isotope was assumed to exist. The group parameters are defined as follows [1,3]:

$$\psi_n^g(Z) = \int_{E_g}^{E_{g-1}} \psi_n(Z, E) dE \tag{III-3}$$

$$\Sigma_t^g(Z) = \frac{\int_{E_g}^{E_{g-1}} \Sigma_t(Z, E) \psi_n(Z, E) dE}{\psi_n^g(Z)} \tag{III-4}$$

$$\chi^g = \int_{E_g}^{E_{g-1}} \chi(E) dE \tag{III-5}$$

$$\nu \Sigma_f^h(Z) = \frac{\int_{E_h}^{E_{h-1}} \nu \Sigma_f(E') \psi_n(Z, E') dE'}{\psi_n^h(Z)} \tag{III-6}$$

$$\Sigma_{sn}^{gh}(Z) = \frac{\int_{E_g}^{E_{g-1}} dE \int_{E_h}^{E_{h-1}} \Sigma_{sn}(Z, E' \rightarrow E) \psi_n(Z, E') dE'}{\psi_n^h(Z)} \tag{III-7}$$

Note the order of subscripts in the scattering cross section  $\Sigma_{sn}^{gh}$  represents scattering from group h to group g.

The angular neutron flux for group  $g$  of the  $P_N$  approximation is found by integrating equation II-3 over the energy group interval, i.e.,  $E_g \leq E \leq E_{g-1}$ , and using the definition given in equation III-3.

$$\psi^g(Z, \mu) = \sum_{n=0}^{\infty} (2n+1) \psi_n^g(Z) P_n(\mu) \quad (\text{III-8})$$

The multigroup  $P_N$  equations with constant neutronic parameters are found from equation III-2.

$$\begin{aligned} n \frac{d}{dZ} \psi_{n-1}^g(Z) + (n+1) \frac{d}{dZ} \psi_{n+1}^g(Z) + \\ (2n+1) \Sigma_t^g \psi_n^g(Z) - (2n+1) \sum_{h=1}^G \alpha_n^{gh} \psi_n^h(Z) = 0 \end{aligned} \quad (\text{III-9})$$

where:

$$\alpha_n^{gh} = \delta_{0n} \frac{1}{\lambda} \chi^{g\nu} \Sigma_f^h + \Sigma_{sn}^{gh} \quad (\text{III-10})$$

(n=0, 1, ..., N)  
(g=1, 2, ..., G)

The next chapter is devoted to the development of the nodal model that is applied to the multigroup  $P_N$  equations given in III-9.

## IV. APPLICATION OF THE NODAL MODEL TO THE MULTIGROUP

 $P_N$  EQUATIONS IN ONE DIMENSION

The technique used in this model is based upon polynomial expansion of the neutron flux within a node. The assumption is that the neutron flux in the  $P_N$  equations can be expressed in the form of a polynomial with Legendre expansions as the trial functions. The least squares technique of the finite element method is used to minimize the residual of the approximate expansions over the node. The unknown polynomial coefficients are then calculated by using the interface fluxes, and the relationships that are obtained from the least squares technique. Using the calculated coefficients, one could find new interface fluxes. Since the fluxes are calculated from the polynomial coefficients and the coefficients in turn from the fluxes, the model requires an iterative process. The iterative scheme to determine the corresponding polynomial coefficients is known as the source iteration method [6].

Since the Legendre polynomials form a complete set of orthogonal functions over the interval  $-1 \leq U \leq +1$ , it would be an incentive to make a change of variable in the multigroup form of the  $P_N$  equations. In doing so, the evaluation of the integrals in the least squares technique is facilitated since one could make use of the orthogonal properties of the Legendre polynomials (see the Appendix).

A. Development of the Multigroup  $P_N$  Equations  
in One-Dimensional Nodal Geometry

The one-dimensional nodal geometry is shown in Figure IV-1.

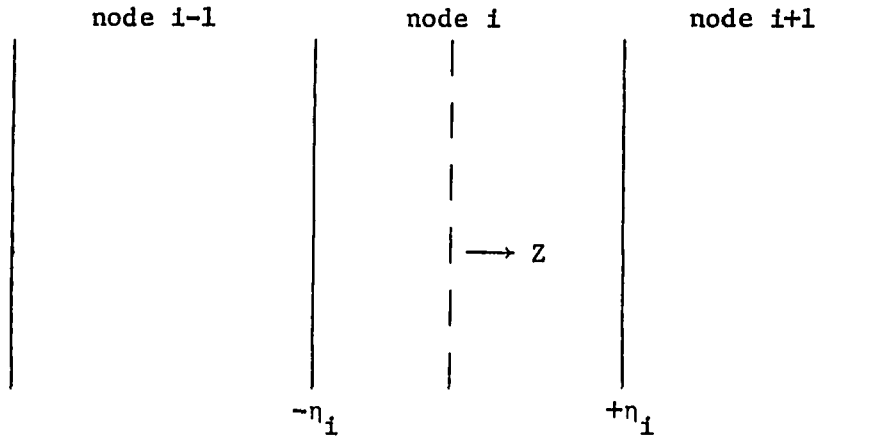


Figure IV-1. One-dimensional nodal geometry

A dimensionless spatial variable defined as:

$$U_i = \frac{Z}{\eta_i} \quad \begin{array}{l} -\eta_i \leq Z \leq +\eta_i \\ -1 \leq U_i \leq +1 \end{array} \quad (\text{IV-1})$$

is used to make a change of variable in the multigroup  $P_N$  equations (III-9) as follow:

$$\begin{aligned} n \frac{d}{dU_i} \psi_{n-1}^g(U_i) + (n+1) \frac{d}{dU_i} \psi_{n+1}^g(U_i) + \\ \eta_i(2n+1) \sum_t^g \psi_n^g(U_i) - \eta_i(2n+1) \sum_{h=1}^G \alpha_n^{gh} \psi_n^h(U_i) = 0 \end{aligned} \quad \begin{array}{l} (n=0,1, \dots, N) \\ (g=1,2, \dots, G) \end{array} \quad (\text{IV-2})$$

Using the dimensionless spatial variable, the angular neutron flux of the  $P_N$  approximation for group  $g$  is found from equation III-8.

$$\psi^g(U_i, \mu) = \sum_{n=0}^N (2n+1) \psi_n^g(U_i) P_n(\mu) \quad (\text{IV-3})$$

The nodal model described in the following sections expands  $\psi_n^g(U_i)$  about the center point of each node. Two sets of Legendre polynomial expansions are used in the model. They are arbitrarily called full and partial expansions and will be discussed in the following sections.

#### B. Theoretical Development for a Full Expansion

The expansion coefficients in equation IV-3 are now expanded in a series of Legendre polynomial:

$$\psi_n^g(U_i) = \sum_{m=0}^M a_{m,n}^g(i) P_m(U_i) \quad \begin{array}{l} M \geq 1 \\ (n=0,1, \dots, N) \\ (g=1,2, \dots, G) \end{array} \quad (\text{IV-4})$$

where  $M$  is the order of the polynomial expansion, and  $a_{m,n}^g(i)$  are the coefficients for group  $g$  of node  $i$ . The angular neutron flux of node  $i$  is found by substituting equation IV-4 into IV-3.

$$\psi^g(U_i, \mu) = \sum_{n=0}^N (2n+1) \sum_{m=0}^M a_{m,n}^g(i) P_m(U_i) P_n(\mu) \quad \begin{array}{l} (g=1,2, \dots, G) \end{array} \quad (\text{IV-5})$$

The expansion in equation IV-4 is called a full expansion since the order of the spatial polynomial remains the same for any order of

angular dependency.

There are  $(N+1)(M+1)$  unknown coefficients in equation IV-5 that must be determined. In order to determine the unknown coefficients, the polynomial expansion (IV-4) and its derivative should be inserted into the  $P_N$  equations (IV-2). Therefore, the derivative of equation IV-4 with respect to  $U_i$  is first found.

$$\frac{d}{dU_i} \psi_n^g(U_i) = \sum_{m=0}^{M-1} b_{m,n}^g(i) P_m(U_i) \quad (\text{IV-6})$$

where the  $b_{m,n}^g(i)$  coefficients are related to the  $a_{m,n}^g(i)$  coefficients through the following expression:

$$b_{m,n}^g(i) = (2m+1) \sum_{k=m+1}^M a_{k,n}^g(i) \quad (\text{IV-7})$$

if  $m$  is even,  $k$  takes only odd values.

if  $m$  is odd,  $k$  takes only even values.

The polynomial expansion (IV-4) and its derivative (IV-6) are now inserted into equation IV-2. Since the polynomial expansion is not the exact solution, a residual is obtained.

$$R_n^g(i) = n \sum_{m=0}^{M-1} b_{m,n-1}^g(i) P_m(U_i) + (n+1) \sum_{m=0}^{M-1} b_{m,n+1}^g(i) P_m(U_i) + \eta_i(2n+1) \sum_t^g \sum_{m=0}^M a_{m,n}^g(i) P_m(U_i) - \eta_i(2n+1) \sum_{m=0}^M c_{m,n}^g(i) P_m(U_i) \quad (\text{IV-8})$$

where:

$$c_{m,n}^g(i) = \sum_{h=1}^G \alpha_n^{gh} a_{m,n}^h(i) \quad (IV-9)$$

(n=0,1, ..., N)  
(g=1,2, ..., G)

The least squares technique (see page 9) is now used to minimize the residuals in equation IV-8 over the nodal interval with respect to the  $b_{m,n}^g(i)$  coefficients. In this process, the minimization is the difference between one of the derivative terms and the rest of the terms (including the other derivative) in equation IV-8. The least squares minimization depends on whether n is even or odd and is carried out as follow:

$$\int_{-1}^{+1} \frac{dR_n^g(i)}{db_{m,n+1}^g(i)} R_n^g(i) \frac{dU_i}{2} = 0 \quad n = \text{even} \quad (IV-10)$$

$$\int_{-1}^{+1} \frac{dR_n^g(i)}{db_{m,n-1}^g(i)} R_n^g(i) \frac{dU_i}{2} = 0 \quad n = \text{odd} \quad (IV-11)$$

(n=0,1, ..., N)  
(m=0, ..., M-1)  
(g=1,2, ..., G)

The relations that result from equations IV-10 and IV-11 are:

$$n b_{m,n-1}^g(i) + (n+1) b_{m,n+1}^g(i) + \eta_i(2n+1) \sum_t a_{m,n}^{gt}(i) = \eta_i(2n+1) c_{m,n}^g(i) \quad (IV-12)$$

(n=0,1, ..., N)  
(m=0, ..., M-1)  
(g=1,2, ..., G)

Since the multigroup  $P_N$  approximation is used to get the relations in

IV-12, the following coefficients should be set equal to zero for  $n = N$ :

$$b_{m,N+1}^g(i) = 0 \quad (\text{IV-13})$$

The orthogonality properties of the Legendre polynomials were used to get the relatively simple relations in equation IV-12.

The relations in IV-12 result in  $(N+1)M$  independent equations. However, an additional  $(N+1)$  independent equations are needed to evaluate the  $(N+1)(M+1)$  polynomial coefficients for group  $g$  of node  $i$ . The interface conditions, which are described in part D of this chapter, are used to obtain the remaining  $(N+1)$  equations.

### C. Theoretical Development for a Partial Expansion

The expansion coefficients in equation IV-3 are now expanded in a series of Legendre polynomial:

$$\psi_n^g(U_i) = \sum_{m=0}^{M-n} a_{m,n}^g(i) P_m(U_i) \quad M \geq N+1 \quad (\text{IV-14})$$

(n=0,1, ..., N)  
(g=1,2, ..., G)

where  $M$  is the order of the polynomial expansion and  $a_{m,n}^g(i)$  are the coefficients for group  $g$  of node  $i$ . The angular neutron flux of node  $i$  is found by substituting equation IV-14 into IV-3:

$$\psi^g(U_i, \mu) = \sum_{n=0}^N (2n+1) \sum_{m=0}^{M-n} a_{m,n}^g(i) P_m(U_i) P_n(\mu) \quad (\text{IV-15})$$

(g=1,2, ..., G)

The expansion in equation IV-14 is called a partial expansion since the order of the spatial polynomial decreases as the order of the angular dependency increases. Therefore, there are fewer unknown polynomial coefficients in the partial expansion as compared to the full expansion development.

There are  $\frac{(2M+2-N)(N+1)}{2}$  unknown coefficients in equation IV-15 that should be determined. In order to determine the unknown coefficients, the same procedure used in the full expansion development is used here. Therefore, the derivative of equation IV-14 with respect to  $U_i$  is first found.

$$\frac{d}{dU_i} \psi_n^g(U_i) = \sum_{m=0}^{M-(n+1)} b_{m,n}^g(i) P_m(U_i) \quad (IV-16)$$

where the  $b_{m,n}^g(i)$  coefficients are related to the  $a_{m,n}^g(i)$  coefficients through the following expression:

$$b_{m,n}^g(i) = (2m+1) \sum_{k=m+1}^{M-n} a_{k,n}^g(i) \quad (IV-17)$$

if  $m$  is even,  $k$  takes only odd values.

if  $m$  is odd,  $k$  takes only even values.

The polynomial expansion (IV-14) and its derivative (IV-16) are now inserted into equation IV-2. Since the polynomial expansion is not the exact solution, a residual is obtained.

$$R_{m,n}^g(i) = n \sum_{m=0}^{M-n} b_{m,n-1}^g(i) P_m(U_i) + (n+1) \sum_{m=0}^{M-(n+2)} b_{m,n+1}^g(i) P_m(U_i) + \eta_i (2n+1) \sum_{m=0}^{M-n} a_{m,n}^g(i) P_m(U_i) - \eta_i (2n+1) \sum_{m=0}^{M-n} c_{m,n}^g(i) P_m(U_i) \quad (IV-18)$$

where  $c_{m,n}^g(i)$  are given in equation IV-9. The least squares technique (see page 9) is now used to minimize the residuals in IV-18 with respect to the  $b_{m,n}^g(i)$  coefficients. In this process, the minimization is the difference between one of the derivative terms and the rest of the terms (including the other derivative) in equation IV-18. The least squares minimization depends on whether  $n$  is even or odd. Since the partial expansion is used, the order of  $m$  is also determined by  $n$  being even or odd. The minimization is carried out as follows:

$$\int_{-1}^{+1} \frac{dR_n^g(i)}{db_{m,n+1}^g(i)} R_n^g(i) \frac{dU_i}{2} = 0 \quad \begin{array}{l} n = \text{even} \\ (m=0, \dots, M-(n+2)) \end{array} \quad (\text{IV-19})$$

$$\int_{-1}^{+1} \frac{dR_n^g(i)}{db_{m,n-1}^g(i)} R_n^g(i) \frac{dU_i}{2} = 0 \quad \begin{array}{l} n = \text{odd} \\ (m=0, \dots, M-n) \end{array} \quad (\text{IV-20})$$

where:

$$\begin{array}{l} (n=0,1, \dots, N) \\ (g=1,2, \dots, G) \end{array}$$

The relations that result from equations IV-19 and IV-20 are:

$$\begin{aligned} n b_{m,n-1}^g(i) + (n+1) b_{m,n+1}^g(i) + \eta_i(2n+1) \sum_t^g a_{m,n}^g(i) = \\ \eta_i(2n+1) c_{m,n}^g(i) \end{aligned} \quad (\text{IV-21})$$

$$\begin{array}{l} (n=0,1, \dots, N) \\ (g=1,2, \dots, G) \end{array}$$

if  $n = \text{even}$ ,  $m = 0, \dots, M-(n+2)$

if  $n = \text{odd}$ ,  $m = 0, \dots, M-n$ ,  $b_{m,n+1}^g = 0$  for  $m > M-(n+2)$

Since the multigroup  $P_N$  approximation is used to get the relations in IV-21, the following coefficients should be set equal to zero for  $n = N$ :

$$b_{m,N+1}^g(i) = 0 \quad (\text{IV-22})$$

The orthogonality properties of the Legendre polynomials were used to get the relatively simple relations in equation IV-21.

The relations in IV-21 result in  $\frac{(2M-N)(N+1)}{2}$  independent equations. However, an additional  $(N+1)$  independent equations are needed to evaluate the  $\frac{(2M+2-N)(N+1)}{2}$  polynomial coefficients for group  $g$  of node  $i$ . The interface conditions, which are described in part D of this chapter, are used to obtain the remaining  $(N+1)$  equations.

#### D. Interface and Boundary Conditions

The interface conditions for the nodal geometry in the dimensionless variable  $U_i$  are shown in Figure IV-2. At various interfaces between different nodes, the angular neutron flux is to be continuous in the direction defined by  $\mu$ . However, it is not possible to satisfy the exact interface conditions since these conditions are imposed over half the angular range, whereas the expansion coefficients apply over the whole range of  $\mu$ , i.e.,  $-1 \leq \mu \leq +1$ .

For the multigroup  $P_N$  approximation,  $(N+1)$  interface conditions

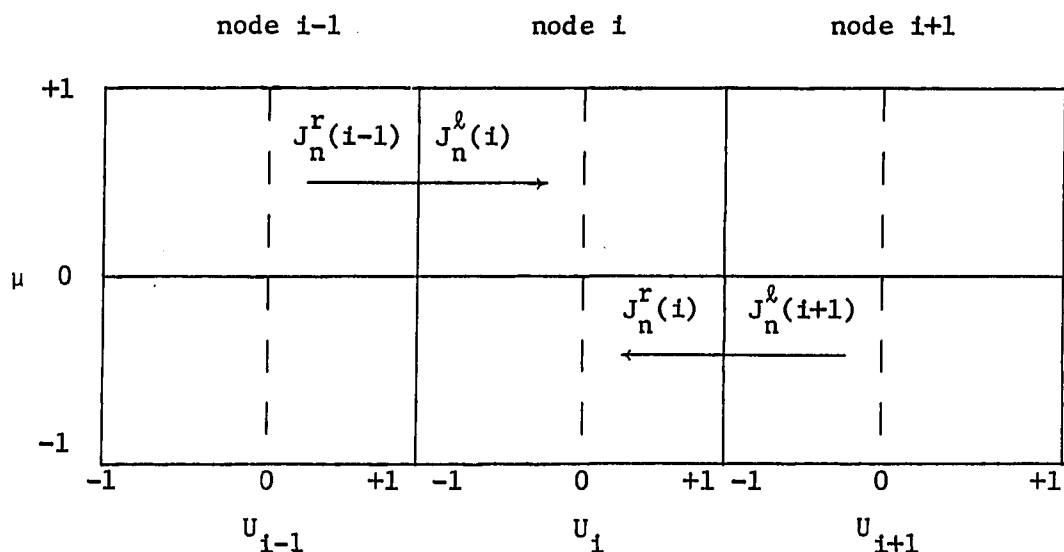


Figure IV-2. Interface conditions for the nodal geometry

are required on the  $(N+1)$  expansion coefficients. Therefore,  $\frac{(N+1)}{2}$  conditions are needed for each interface. For an odd order  $P_N$  approximation, the moments of the angular neutron flux of a given node are assumed to be functions of the properties of that node, and the moments of the angular neutron flux entering that node from adjacent nodes. Therefore, the following interface conditions are used for node  $i$ :

$$\int_{-1}^0 \frac{d\mu}{2} P_n(\mu) \psi_n^g(U_i, \mu) \Big|_{U_i=+1} = J_n^g(i+1) \quad (\text{IV-23})$$

$$\int_0^{+1} \frac{d\mu}{2} P_n(\mu) \psi_n^g(U_i, \mu) \Big|_{U_i=-1} = J_n^g(i-1) \quad (\text{IV-24})$$

$$\begin{aligned} (n=1, 3, \dots, N) \\ (g=1, 2, \dots, G) \end{aligned}$$

where  $J_n^g(i+1)$  and  $J_n^g(i-1)$  are scalar quantities that are evaluated by the following relations, using the values from the previous iteration.

$$J_n^g(i+1) = \int_{-1}^0 \frac{d\mu}{2} P_n(\mu) \psi_n^g(U_{i+1}, \mu) \Big|_{U_{i+1}=-1} \quad (\text{IV-25})$$

$$J_n^g(i-1) = \int_0^{+1} \frac{d\mu}{2} P_n(\mu) \psi_n^g(U_{i-1}, \mu) \Big|_{U_{i-1}=+1} \quad (\text{IV-26})$$

The interface conditions given in equations IV-23 and IV-24 are justified on the basis that for  $n=1$ , the continuity of the current at the interface is insured.

At the interface between a node and an external boundary, two boundary conditions are considered: vacuum, and symmetric boundary conditions. The external boundary condition is either next to node ( $i=1$ ), or the last node ( $i=I$ ). Since the form of equations IV-23 and IV-24 remains the same except for the values of  $J_n^g(i+1)$ , and  $J_n^g(i-1)$ , then  $J_n^g(I+1)$  and  $J_n^g(0)$  are used to represent the boundaries next to node ( $i=I$ ) and ( $i=1$ ). Note that nodes ( $i=I+1$ ) and ( $i=0$ ) do not exist.

At an interface next to a vacuum, the Marshak boundary conditions are used, where  $J_n^g(I+1)$  and  $J_n^g(0)$  are set equal to zero [1].

$$J_n^g(I+1) = 0 \quad (\text{IV-27})$$

$$J_n^g(0) = 0 \quad (\text{IV-28})$$

$$\begin{aligned} & (n=1, 3, \dots, N) \\ & (g=1, 2, \dots, G) \end{aligned}$$

The Marshak boundary conditions are justified on the basis that the condition for  $n=1$  is the  $P_N$  expression for zero returning net current [1].

At an interface next to a symmetric boundary  $J_n^g(I+1)$ , and  $J_n^g(0)$  are evaluated by the following relations.

$$J_n^g(I+1) = - \int_0^{+1} \frac{d\mu}{2} P_n(\mu) \psi_n^g(U_I, \mu) \Big|_{U_I=+1} \quad (\text{IV-29})$$

$$J_n^g(0) = - \int_{-1}^0 \frac{d\mu}{2} P_n(\mu) \psi_n^g(U_1, \mu) \Big|_{U_1=-1} \quad (\text{IV-30})$$

$$\begin{aligned} & (n=1, 3, \dots, N) \\ & (g=1, 2, \dots, G) \end{aligned}$$

The application of the interface and boundary conditions is facilitated by the following half range relations [18]:

$$\int_0^{+1} P_m(\mu) P_n(\mu) \frac{d\mu}{2} \quad (\text{IV-31})$$

$$= \begin{cases} \frac{1}{2(2m+1)} & \text{if } m = n \\ 0 & \text{if } m-n \text{ is even} \\ & (m-n \neq 0) \\ \frac{(-1)^{i+k} m! n!}{2^{m+n} (n-m)(n+m+1)(i!)^2 (k!)^2} & \text{if } m = 2k, \text{ and} \\ & n = 2i+1 \end{cases}$$

$$\int_{-1}^0 P_m(\mu) P_n(\mu) \frac{d\mu}{2} \quad (\text{IV-32})$$

$$= \begin{cases} \frac{1}{2(2m+1)} & \text{if } m = n \\ 0 & \text{if } m-n \text{ is even} \\ & (m-n \neq 0) \\ \frac{(-1)^{i+k+1} m! n!}{2^{m+n} (n-m)(n+m+1)(i!)^2 (k!)^2} & \text{if } m = 2k, \text{ and} \\ & n = 2i+1 \end{cases}$$

The (N+1) interface conditions of node  $i$  complete the specification for group  $g$  of the multigroup  $P_N$  approximation. Therefore, for any energy group and node, enough independent equations are available to solve for the unknown coefficients of the angular neutron flux.

#### E. Derivation of the Effective Multiplication Factor

Finally, the effective multiplication factor should be found using the calculated polynomial coefficients. Two different procedures are used in finding the effective multiplication factor. The first of these applies a neutron balance over all of the nodes and neutron groups. The neutron balance as applied to the multigroup  $P_N$  equations (IV-2) is:

$$\sum_{i=1}^I \sum_{g=1}^G \int_{-1}^{+1} \left\{ \frac{d}{dU_i} \psi_1^g(U_i) + \eta_i \Sigma_t^g \psi_0^g(U_i) - \eta_i \sum_{h=1}^G \left[ \frac{1}{\lambda_1} \chi^g \nu \Sigma_f^h + \Sigma_{s0}^{gh} \psi_0^h(U_i) \right] \right\} \frac{dU_i}{2} = 0 \quad (\text{IV-33})$$

The nodal average fluxes are just the first coefficients of the expansion because of the orthogonality of the Legendre polynomials:

$$\bar{\psi}_0^g(U_i) = \int_{-1}^{+1} \psi^g(U_i) \frac{dU_i}{2} = a_{0,0}^g(i) \quad (\text{IV-34})$$

The value of the expansion coefficients at the nodal interfaces are needed as a result of the integration of the leakage term. These values depend on whether the full or partial expansions are used:

$$\psi_1^g(U_i) \Big|_{U_i=+1} - \psi_1^g(U_i) \Big|_{U_i=-1} = \sum_{k=1}^K a_{k,1}^g(i) \quad (\text{IV-35})$$

if full expansion is used,  $K = M$

if partial expansion is used,  $K = M-1$

in both cases,  $k$  takes only odd values

where  $M$  is the order of the polynomial expansion.

Solving for the eigenvalue and applying equations IV-34 and IV-35, one has:

$$\lambda_1^j = \frac{\left\{ \sum_{i=1}^I \sum_{g=1}^G \sum_{h=1}^G \eta_i \chi^g \nu \Sigma_f^h a_{0,0}^h(i) \right\}^j}{\left\{ \sum_{i=1}^I \sum_{g=1}^G \left[ \sum_{k=1}^K a_{k,1}^g + \eta_i \Sigma_t^g a_{0,0}^g(i) - \eta_i \sum_{h=1}^G \Sigma_{s0}^{gh} a_{0,0}^h(i) \right] \right\}^j} \quad (\text{IV-36})$$

where  $K$  is defined in equation IV-35 for the full and partial expansions, and  $j$  represents the iteration number.

The second procedure estimates the effective multiplication factor by using its value from the previous iteration and the values of the nodal average fluxes [6].

$$\lambda_2^j = \frac{\lambda^{j-1} \left[ \sum_{i=1}^I \sum_{g=1}^G \sum_{h=1}^G \eta_i \chi_{\nu \Sigma_f}^{g,h,h} a_{0,0}^{(i)} \right]^j}{\left[ \sum_{i=1}^I \sum_{g=1}^G \sum_{h=1}^G \eta_i \chi_{\nu \Sigma_f}^{g,h,h} a_{0,0}^{(i)} \right]^{j-1}} \quad (\text{IV-37})$$

Note that either one of the calculated effective multiplication factors could be used in the iterative process, since the two should become equal when a converged solution has been attained. This would serve as a tool for monitoring the convergence of the solution. In summary, the relations obtained from the least squares minimization along with the interface and boundary conditions are used to evaluate the unknown polynomial coefficients. Using the calculated coefficients, the effective multiplication factor and new interface fluxes are evaluated. An iteration technique is then applied until convergence is obtained.

## V. COMPUTER PROGRAM, SAMPLE PROBLEMS, AND RESULTS

A computer program called TONODE [19] was developed to test the nodal model for accuracy of solution. The program is a one-dimensional multigroup code capable of handling up to  $P_5$  approximations using both full and partial expansions. The fourth-order Legendre polynomial is used in the code since it was observed by Rohach [5] that this polynomial order is enough for normal reactor problems. Two sample problems were developed to compare the results of the nodal model with the results of more accurate models.

### A. $P_1$ Approximation for a Full and Partial Expansion

The multigroup  $P_1$  equations for group  $g$  of node  $i$  are obtained from equation IV-2.

$$\frac{d}{dU_i} \psi_1^g(U_i) + \eta_i \Sigma_t^g \psi_0^g(U_i) - \eta_i \sum_{h=1}^G \alpha_0^{gh} \psi_0^h(U_i) = 0 \quad (V-1)$$

$$\frac{d}{dU_i} \psi_0^g(U_i) + 3\eta_i \Sigma_t^g \psi_1^g(U_i) - 3\eta_i \sum_{h=1}^G \alpha_1^{gh} \psi_1^h(U_i) = 0 \quad (V-2)$$

A sample problem was developed for comparison with a one-dimensional version of the ANL Benchmark problem [20]. The fuel loading pattern with symmetric boundary condition at the left, and vacuum boundary condition at the right, is shown in Figure V-1. The cross section data used for the fuel types in Figure V-1 are given in Table V-1.

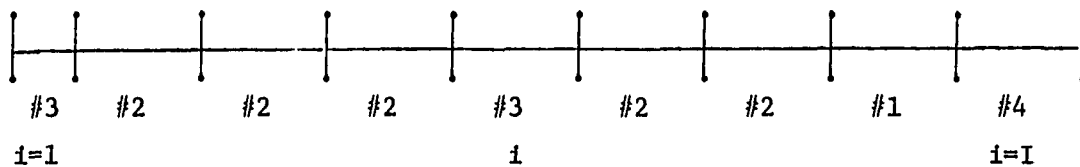


Figure V-1. Fuel loading pattern for the one-dimensional model, problem 1

Table V-1. Benchmark fuel parameters

Material	Region	$D^1$	$D^2$	$\Sigma_{s0}^{21}$	$\Sigma_a^1$	$\Sigma_a^2$	$\nu\Sigma_f^2$
Fuel 1	#1	1.5	0.4	0.02	0.01	0.08	0.135
Fuel 2	#2	1.5	0.4	0.02	0.01	0.085	0.135
Fuel 2 & Control	#3	1.5	0.4	0.02	0.01	0.13	0.135
Reflector	#4	2.0	0.3	0.04	0.0	0.01	0.0

where  $D^g$  is the diffusion coefficient for group  $g$ , and is used to calculate  $\Sigma_{s1}^{gg}$ .

$$\Sigma_{s1}^{gg} = \Sigma_t^g - \frac{1}{3D^g} \quad (V-3)$$

and  $\Sigma_{s1}^{gh}$  is assumed to be zero for  $h \neq g$ .

The node size used in the model is 20 cm except for the first node which is 10 cm. A fine mesh finite difference theory calculation was used for comparison. A comparison of the fast and thermal flux profiles of the fine mesh calculation with the full and partial expansions are shown in Figures V-2 and V-3. As it is observed, the solution of

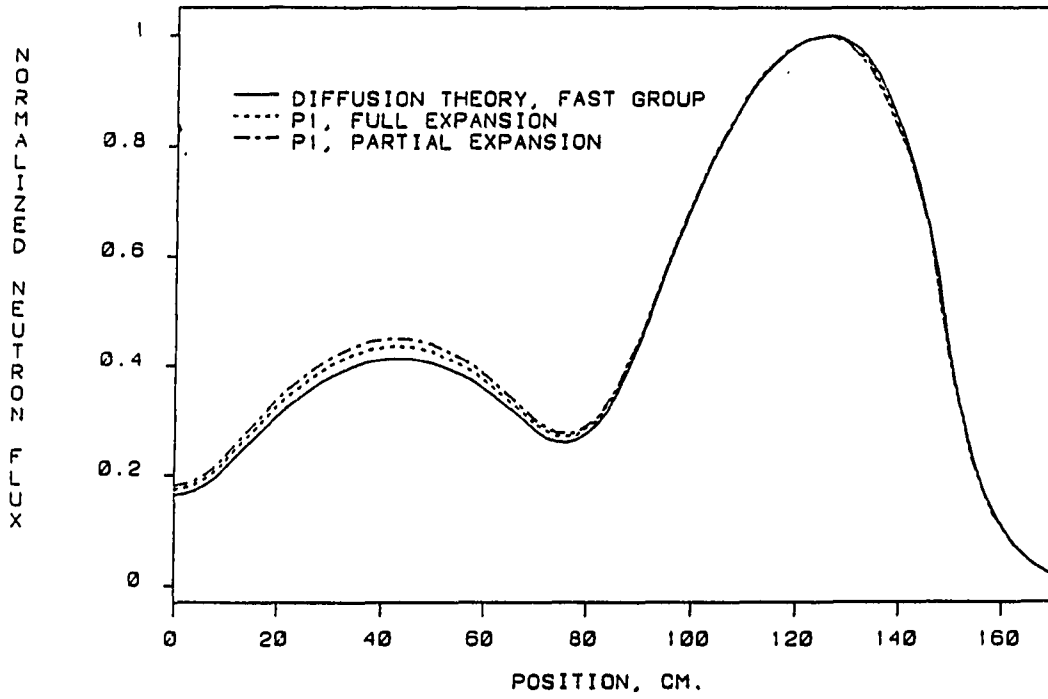


Figure V-2. Fast flux profiles for sample problem one

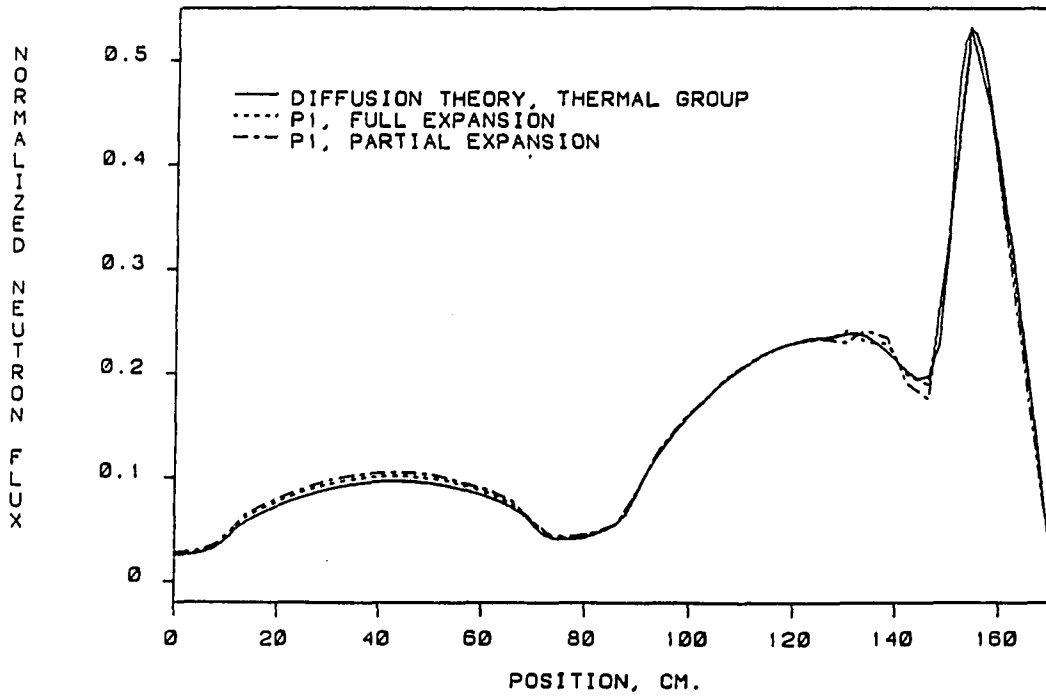


Figure V-3. Thermal flux profiles for sample problem one

the nodal model using a full expansion is closer to the fine mesh diffusion theory calculations than the solution of the partial expansion. This is more apparent in the thermal flux profiles where a large flux peaking occurs in the reflector. However, it should be noted that the solution of the nodal model does not match the fine mesh diffusion theory calculations at the fuel-reflector interface node. This point is illustrated when one compares the derivative terms and the rest of the terms in equations V-1 and V-2.

For a full expansion, the least squares technique minimizes the difference between a third-order polynomial (the derivative term) and a fourth-order polynomial (the rest of the terms) in equations V-1 and V-2. The derivative term and the rest of the terms in equations V-1 and V-2 are shown in Figures V-4 and V-5 for the thermal group of the full expansion, and as it is observed the minimization is quite good. However, the least squares technique has trouble minimizing the difference between the third-order derivative and the remaining fourth-order polynomials at the region of large flux gradients.

For a partial expansion, the derivative terms have different orders of polynomial. The derivative in equation V-1 is a second-order polynomial, whereas the derivative in equation V-2 is a third-order polynomial. Note that the rest of the terms in equations V-1 and V-2 are fourth-order polynomials.

The derivative term and the rest of the terms in equation V-1 are shown in Figure V-6 for the thermal group of the partial expansion. It is observed that the error in the minimization is much more severe than

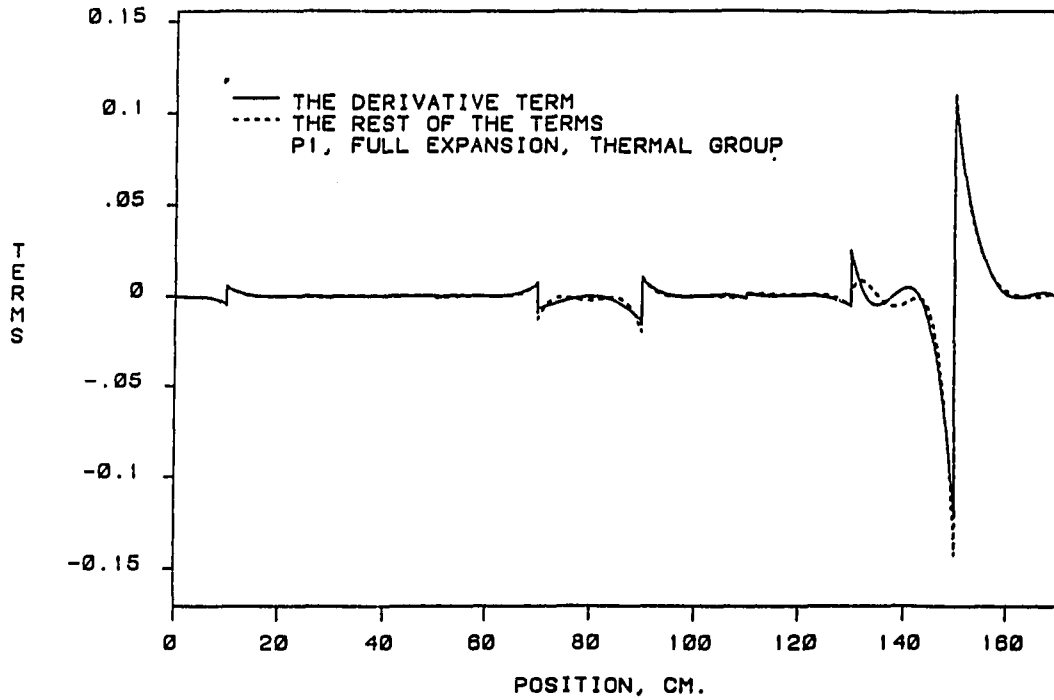


Figure V-4. Magnitude of the relative terms in equation V-1 for sample problem one, using a full expansion

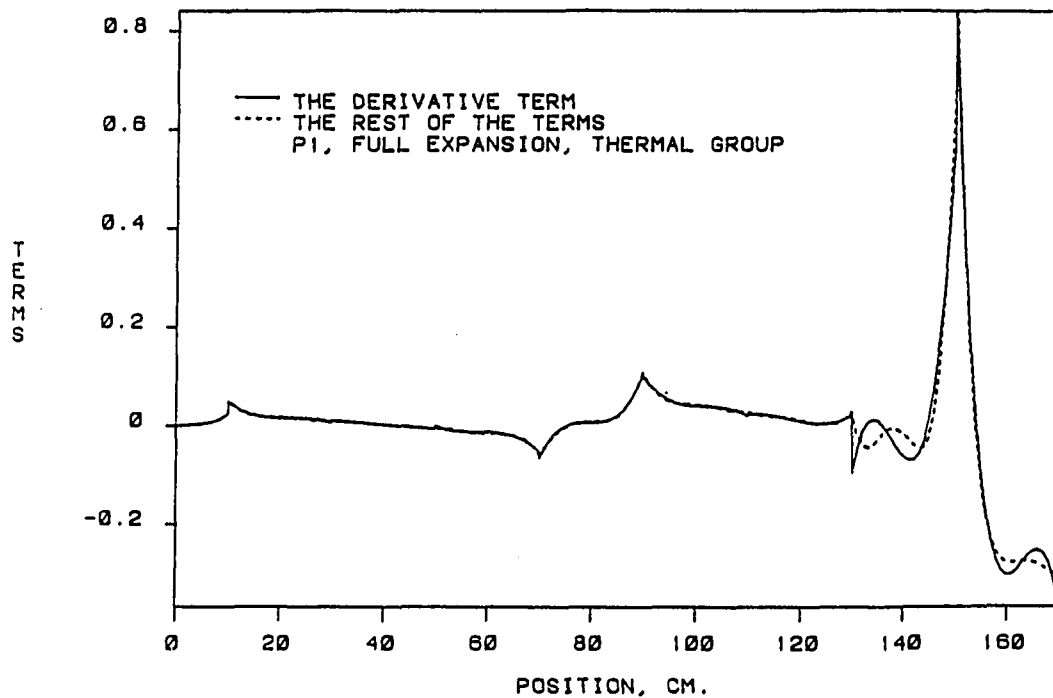


Figure V-5. Magnitude of the relative terms in equation V-2 for sample problem one, using a full expansion

the one for the full expansion. This is due to the fact that the least squares technique has trouble minimizing the difference between the second-order derivative and the remaining fourth-order polynomials.

Figure V-7 shows the derivative term and the rest of the terms in equation V-2 for the thermal group of the partial expansion. It is observed that there is no error in the least squares minimization which is due to the fact that the third-order approximation to the derivative term completely matches the remaining third-order polynomials in equation V-2.

The neutron current, which is the  $P_1$  weight of the angular neutron flux, is required to be continuous at the nodal interfaces. A comparison of the currents for the fast and thermal groups of the full and partial expansions are shown in Figures V-8 and V-9. It is observed that the neutron currents for both expansions are indeed continuous at the nodal interfaces. It is also noted that the neutron currents for both expansions are similar inside the core but deviate from each other at the core-reflector interface node. This is due to the fact that the partial expansion has one less term in its polynomial series than the full expansion.

Finally, when a converged solution of the  $P_1$  equations has been found, the angular neutron flux of node  $i$  could be obtained from equation IV-3:

$$\psi^g(U_i, \mu) = \psi_0^g(U_i) P_0(\mu) + 3\psi_1^g(U_i) P_1(\mu) \quad (V-4)$$

(g=1,2, ..., G)

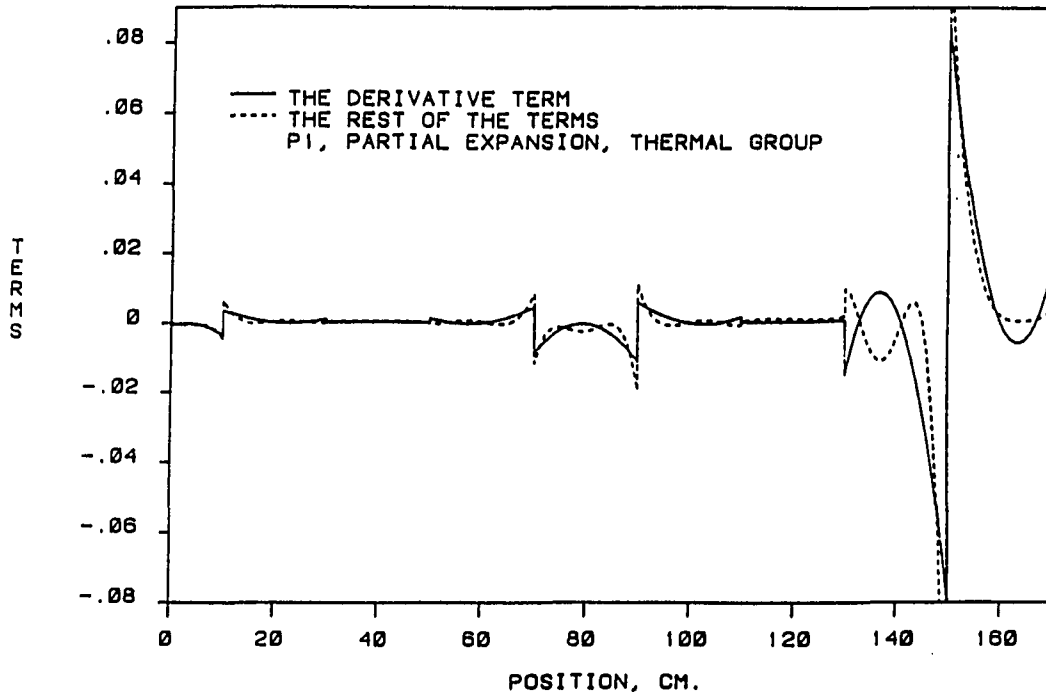


Figure V-6. Magnitude of the relative terms in equation V-1 for sample problem one, using a partial expansion

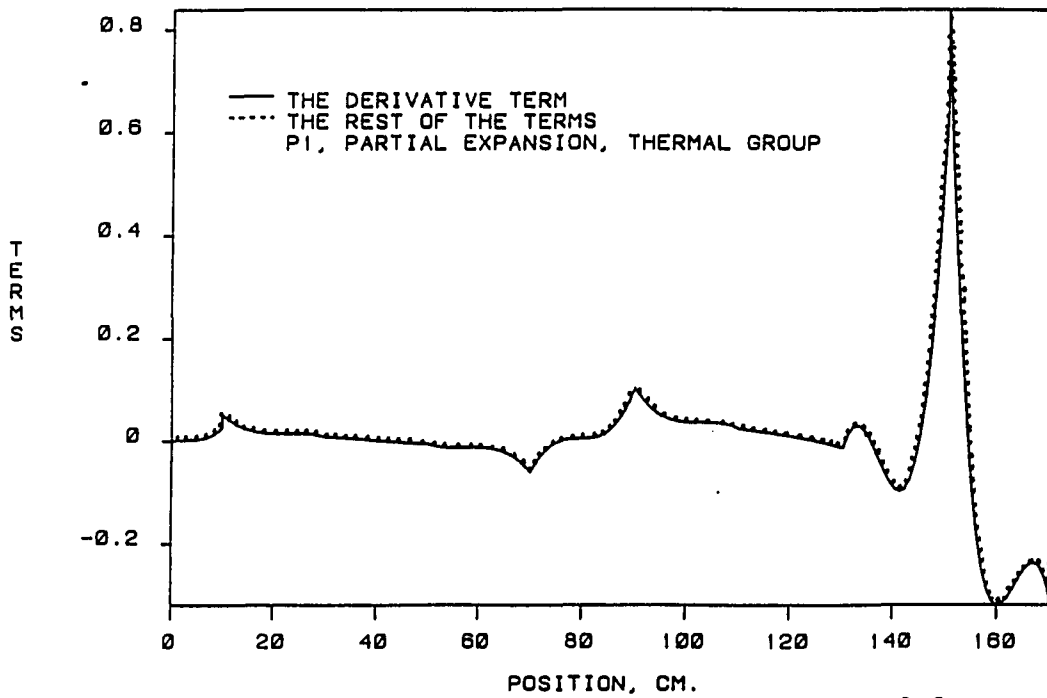


Figure V-7. Magnitude of the relative terms in equation V-2 for sample problem one, using a partial expansion

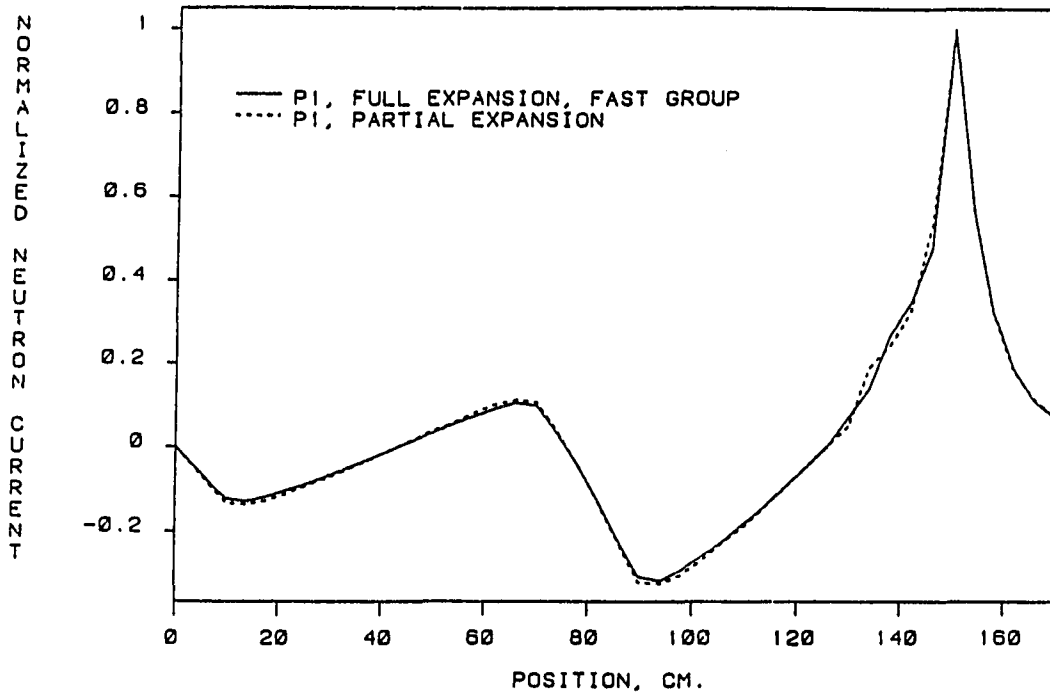


Figure V-8. Fast current profiles for sample problem one

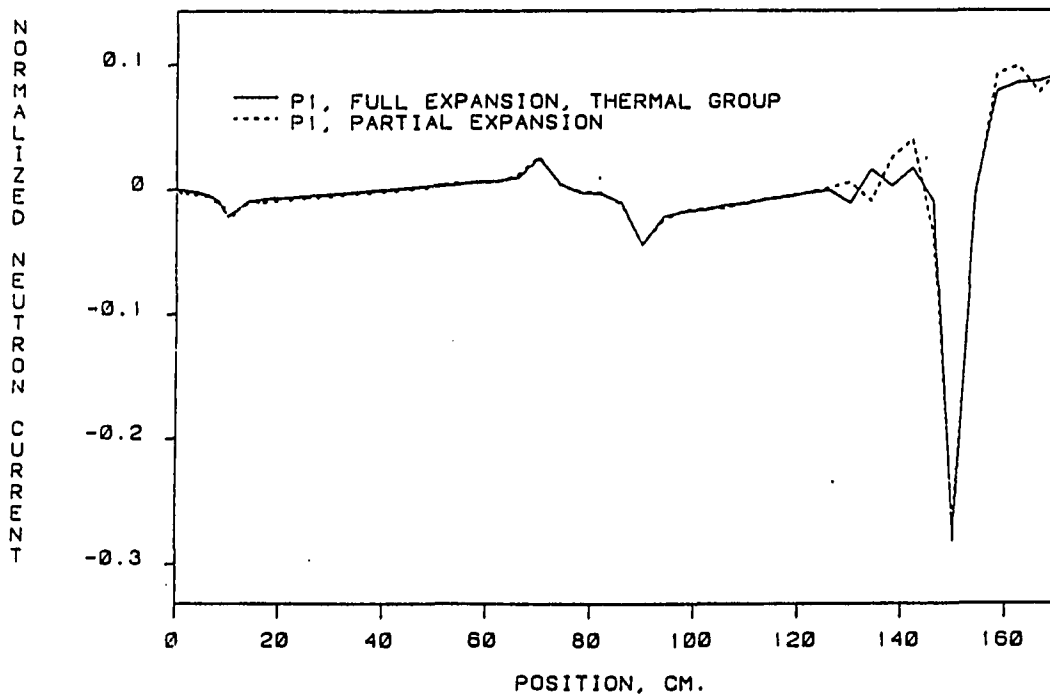


Figure V-9. Thermal current profiles for sample problem one

The sample problem presented here illustrates that for the partial expansion, the least squares technique has trouble minimizing the difference between the second-order derivative term and the remaining fourth-order polynomial terms in the first equation of the  $P_1$  approximation. As a result, when the order of the  $P_N$  approximation increases, the error in the minimization would increase which would in turn defeat using higher order  $P_N$  equations. Therefore, it is concluded that the partial expansion should only be used in developing low  $P_N$  equations, and in regions where large flux gradients do not occur. On the other hand, the full expansion is adequate in predicting an accurate solution for the  $P_N$  equations, except in nodes where severe flux gradients occur. In these cases, it may be necessary to increase the number of nodes to get a better match between the third-order derivative and the fourth-order terms.

The significance of this sample problem was basically to test the model for cases where diffusion theory is valid. The diffusion theory would be a poor approximation whenever the angular distribution of the neutrons is large in one preferred direction. This can happen near an interface where scattering or the absorption cross section changes abruptly. To test the nodal model for cases where diffusion theory is not valid, a second sample problem was developed and is discussed in the following section.

B.  $P_3$  and  $P_5$  Approximations for a Full Expansion

To test the nodal model for cases where an explicit accounting of the transport theory effects are important, a second sample problem was developed. To compare the results of the model with a more accurate model, a transport theory discrete ordinates program called TODMG and a set of three group cross sections were developed by Rohach [21]. The cross section data are given in Table V-2. It is noted that the cross

Table V-2. Nuclear fuel data

Region:	Fuel 1	Fuel 2
	#1	#2
$D^1$	0.18169E+01	0.18169E+01
$D^2$	0.79400E+00	0.79400E+00
$D^3$	0.37071E+00	0.37071E+00
$\Sigma_a^1$	0.35245E-02	0.35245E-02
$\Sigma_a^2$	0.28910E-01	0.28910E-01
$\Sigma_a^3$	0.80027E-01	0.80027E+00
$\nu\Sigma_f^1$	0.42628E-02	0.42628E-02
$\nu\Sigma_f^2$	0.12215E-01	0.12215E-01
$\nu\Sigma_f^3$	0.13514E+00	0.13514E+00
$\Sigma_s^{21}$	0.33652E-01	0.33652E-01
$\Sigma_s^{31}$	0.52783E-01	0.52783E-01

sections in regions #1 and #2 are exactly the same except for the thermal absorption cross section of region #2, which is higher than the thermal absorption cross section of region #1 by a factor of 10.

A sample problem was developed to test the  $P_3$  and  $P_5$  approximations of the nodal model using the cross sections in Table V-2. The multigroup  $P_5$  equations for group  $g$  of node  $i$  are obtained from equation IV-2:

$$\frac{d}{dU_i} \psi_1^g(U_i) + \eta_i \Sigma_t^g \psi_0^g(U_i) - \eta_i \sum_{h=1}^G \alpha_0^{gh} \psi_0^h(U_i) = 0 \quad (V-5)$$

$$\begin{aligned} \frac{d}{dU_i} \psi_0^g(U_i) + 2 \frac{d}{dU_i} \psi_2^g(U_i) + 3 \eta_i \Sigma_t^g \psi_1^g(U_i) \\ - 3 \eta_i \sum_{h=1}^G \alpha_1^{gh} \psi_1^h(U_i) = 0 \end{aligned} \quad (V-6)$$

$$3 \frac{d}{dU_i} \psi_3^g(U_i) + 2 \frac{d}{dU_i} \psi_1^g(U_i) + 5 \eta_i \Sigma_t^g \psi_2^g(U_i) = 0 \quad (V-7)$$

$$3 \frac{d}{dU_i} \psi_2^g(U_i) + 4 \frac{d}{dU_i} \psi_4^g(U_i) + 7 \eta_i \Sigma_t^g \psi_3^g(U_i) = 0 \quad (V-8)$$

$$5 \frac{d}{dU_i} \psi_5^g(U_i) + 4 \frac{d}{dU_i} \psi_3^g(U_i) + 9 \eta_i \Sigma_t^g \psi_4^g(U_i) = 0 \quad (V-9)$$

$$5 \frac{d}{dU_i} \psi_4^g(U_i) + 11 \eta_i \Sigma_t^g \psi_5^g(U_i) = 0 \quad (V-10)$$

where  $\Sigma_{s1}^{gg}$  is calculated from equation V-3, and  $\Sigma_{s1}^{gh}$  for  $h \neq g$  along with  $\Sigma_{sn}^{gh}$  for  $n \geq 2$  are set equal to zero. The multigroup  $P_3$  equations could be obtained by using the first four equations of the  $P_5$  approximation, and setting the derivative of  $\psi_4^g(U_i)$  equal to zero.

The fuel loading pattern with symmetric boundary conditions is shown in Figure V-10, where the node size for region #1 was 0.5 cm, and

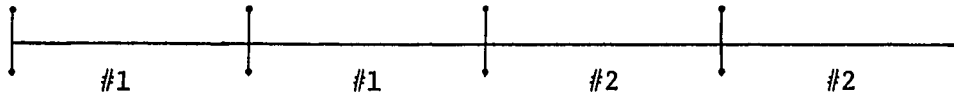


Figure V-10. Fuel loading pattern for the one-dimensional model, problem 2

for region #2 was 1.9 cm. The transport theory program using a fine mesh finite difference calculation with a sixth order Gaussian quadrature was used for comparison. A comparison of the thermal flux profiles of the transport program with the  $P_3$  and  $P_5$  approximations of the nodal model using the full expansion is shown in Figure V-11. As it is observed, the solutions of the nodal model are very close to the discrete ordinate solution of the neutron transport equation. The solution of the problem using a full expansion  $P_1$  approximation is also shown in Figure V-11. As one can see, the solution of the  $P_1$  approximation is not as good as the solution of the  $P_3$  or the  $P_5$  approximations. This is due to the fact that the thermal absorption cross section at the interface between region #1 and region #2 changes abruptly, a case where the  $P_1$  approximation would be poor.

In order to insure the accuracy of the solution, one could compare the derivative term that is being minimized by the least squares technique with the rest of the terms (including the other derivative) in equations V-5 through V-10. Note that in obtaining the  $P_3$  and  $P_5$

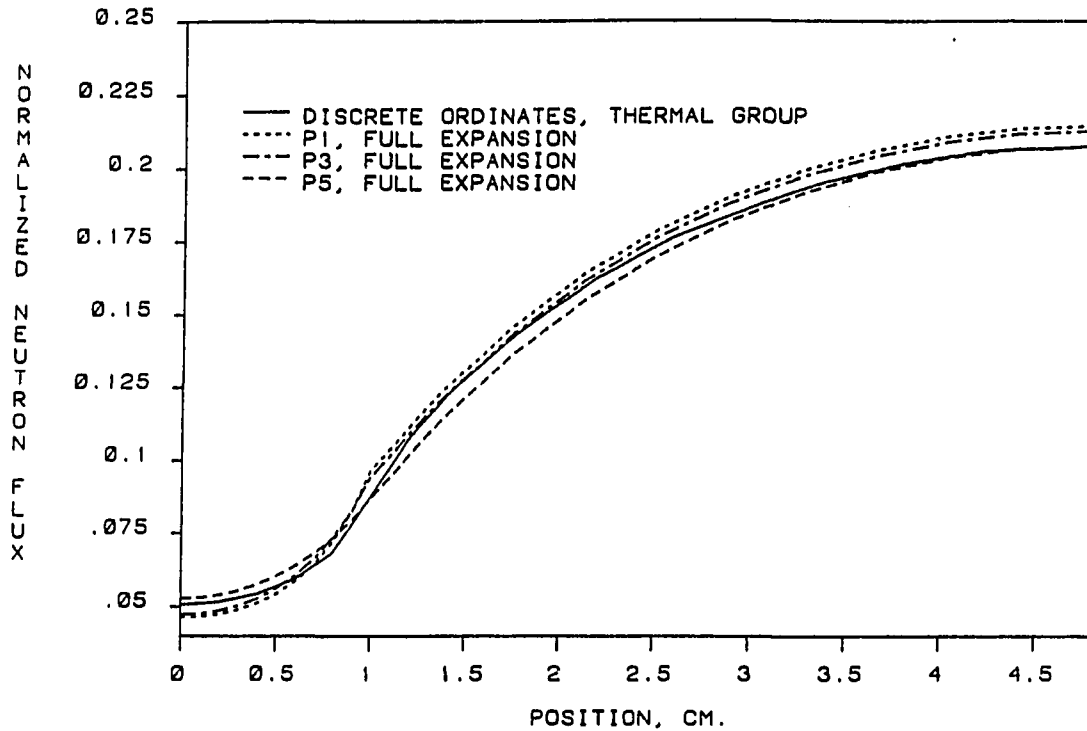


Figure V-11. Thermal flux profiles for sample problem two

equations, the equations were rearranged such that the derivative that is being minimized by the least squares technique appears first in each equation. Since the full expansion of the nodal model is used in this sample problem, the derivative terms are third-order polynomials, whereas the rest of the terms are fourth-order polynomials. The derivative term that is being minimized and the rest of the terms (including the other derivative) in equations V-5 through V-10 are shown in Figures V-12 through V-17 for the thermal group of the  $P_3$  and  $P_5$  approximations. As one can see, the least squares minimization is quite good for both approximations such that the third-order derivative term and the remaining fourth-order polynomials fall on the top of each

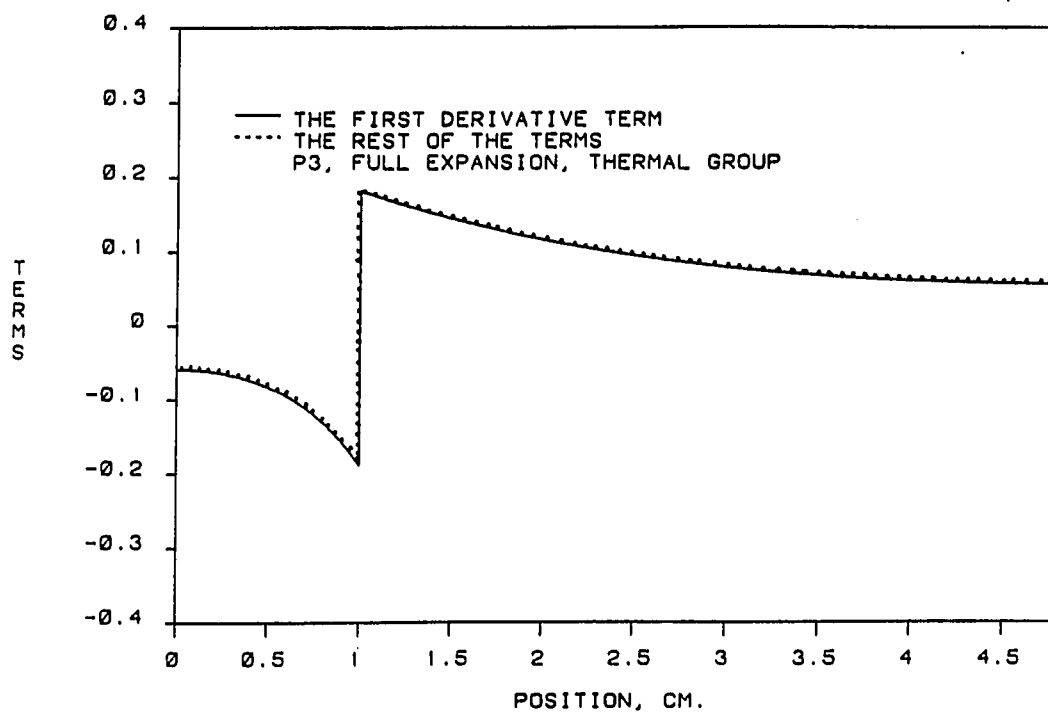


Figure V-12. Magnitude of the relative terms in equation V-5 for sample problem two

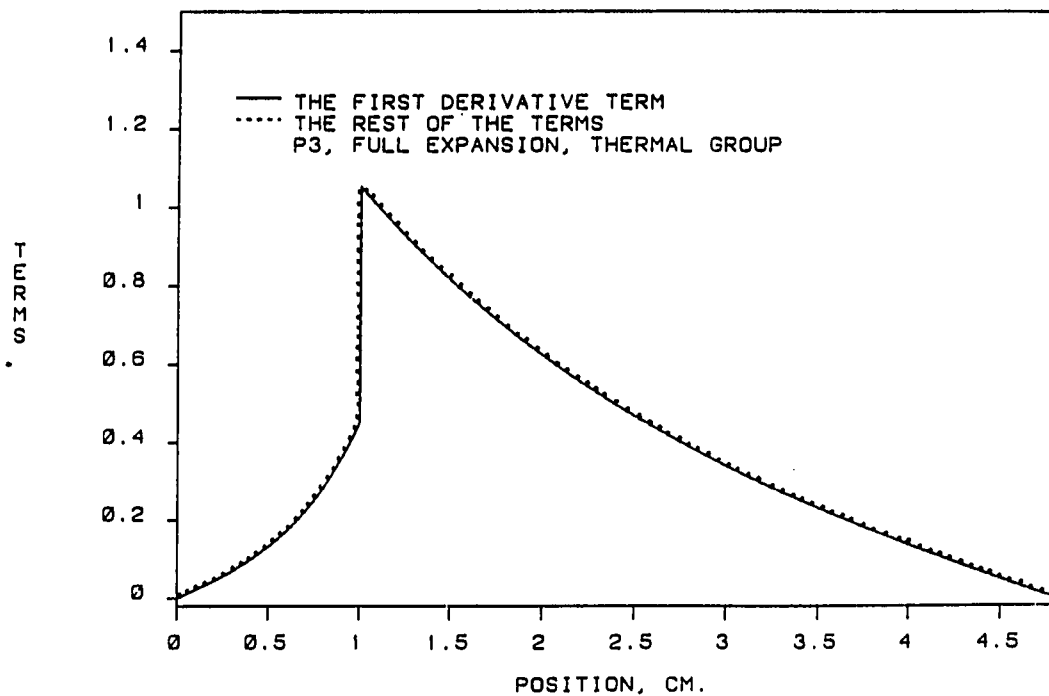


Figure V-13. Magnitude of the relative terms in equation V-6 for sample problem two

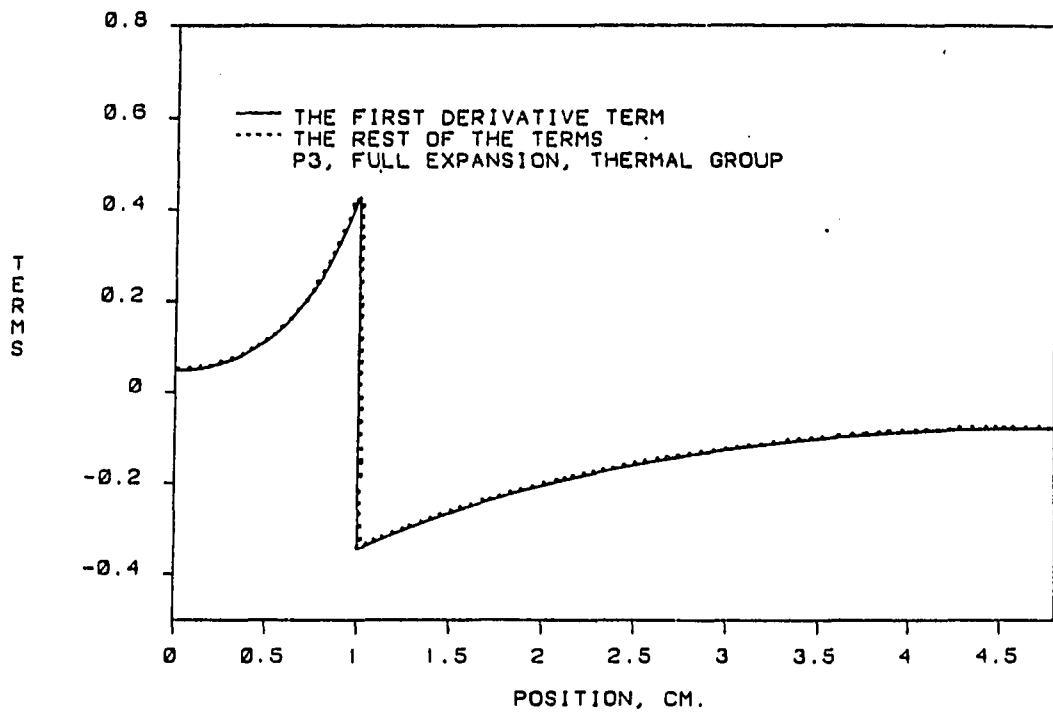


Figure V-14. Magnitude of the relative terms in equation V-7 for sample problem two

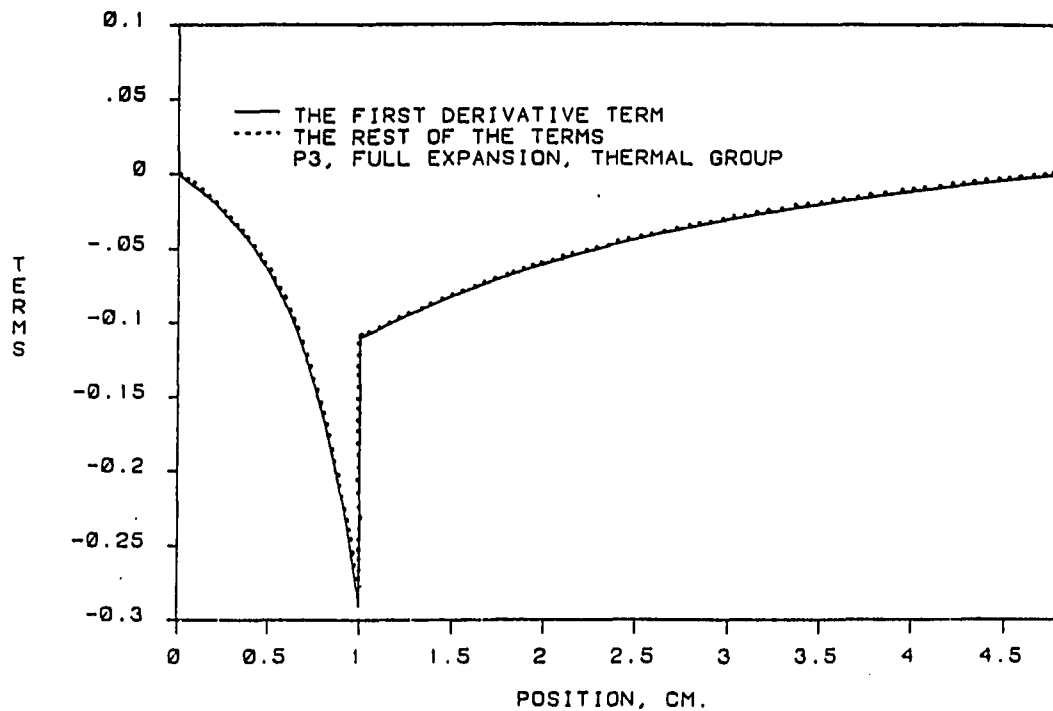


Figure V-15. Magnitude of the relative terms in equation V-8 for sample problem two

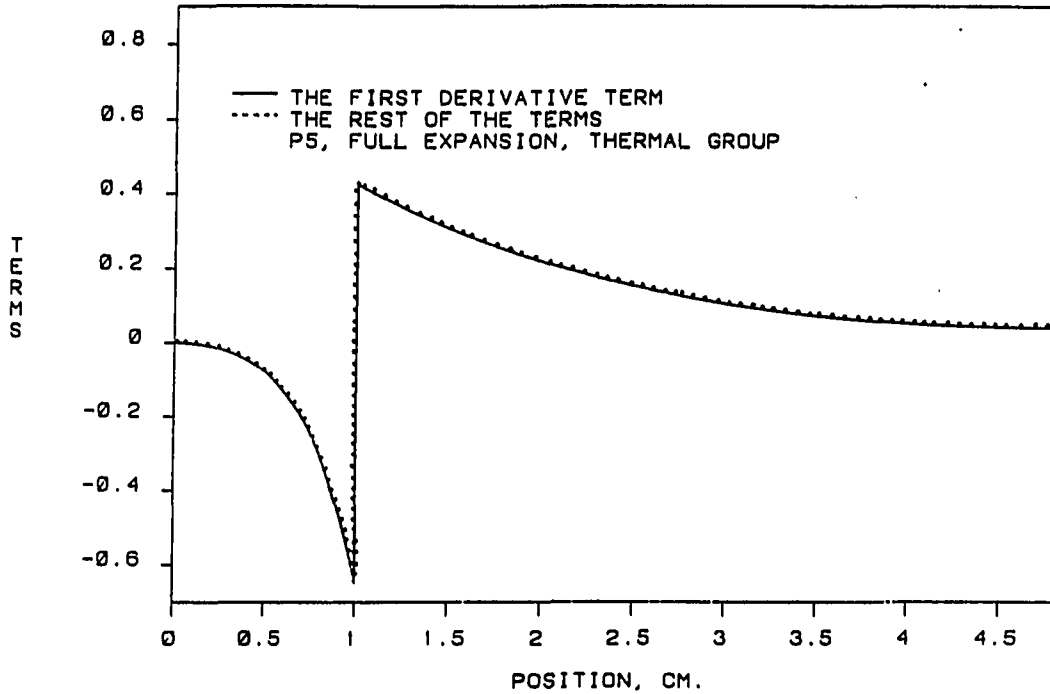


Figure V-16. Magnitude of the relative terms in equation V-9 for sample problem two

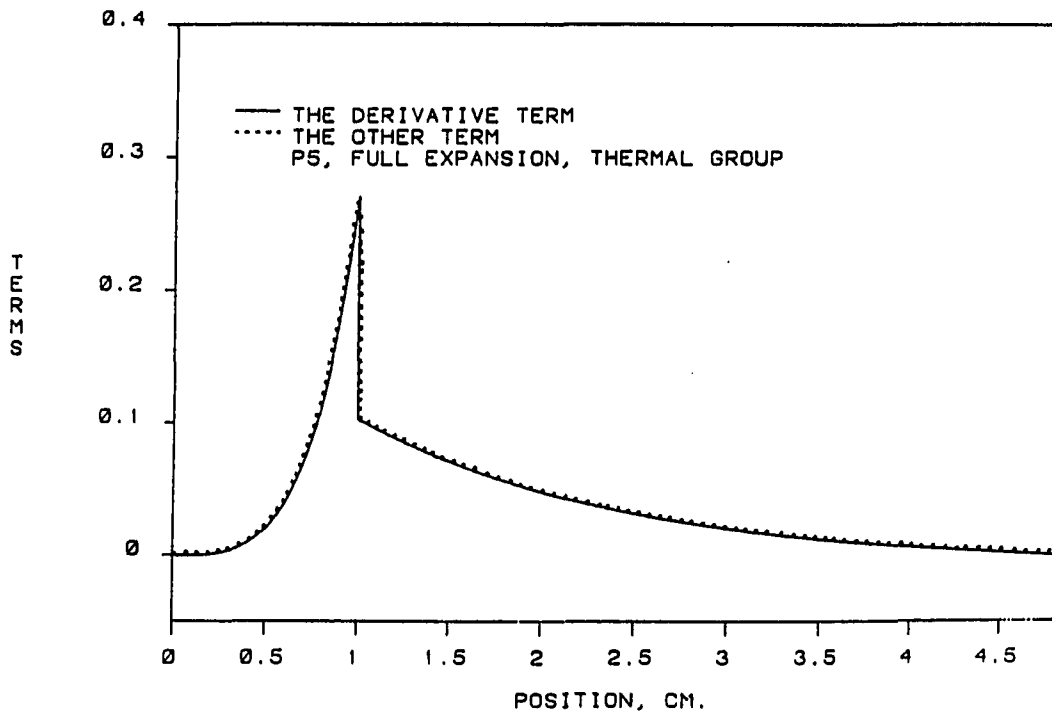


Figure V-17. Magnitude of the relative terms in equation V-10 for sample problem two

other and only one set of curves is seen in each graph. This observation leads to the conclusion that for the given sample problem, the  $P_3$  approximation is enough and the higher  $P_5$  approximation is not necessary. However, the results of this sample problem insure the accuracy of the  $P_5$  approximation of the nodal model.

Another criterion that could be used in order to insure the accuracy of the solution is to illustrate the moments of the angular neutron flux at the nodal interfaces over the whole range of  $\mu$ , i.e.,  $-1 \leq \mu \leq +1$ . It is recalled from the interface conditions that only the odd moments of the angular neutron flux were required to be continuous and that was imposed over half the angular range. Therefore, for the  $P_3$  approximation, the  $P_1$ ,  $P_2$ , and  $P_3$  weights of the angular neutron flux should be continuous at the nodal interfaces. For the  $P_5$  approximation, the  $P_1$ ,  $P_2$ ,  $P_3$ ,  $P_4$ , and  $P_5$  weights of the angular neutron flux should be continuous at the nodal interfaces. Figures V-18 through V-20 show the  $P_1$ ,  $P_2$ , and  $P_3$  weights of the angular neutron flux for the thermal group of the  $P_3$  and  $P_5$  approximations. Figures V-21 and V-22 show the  $P_4$  and  $P_5$  weights of the angular neutron flux for the  $P_5$  approximation. It is observed that the weights of the angular neutron flux for both the  $P_3$  and  $P_5$  approximations are continuous at the interfaces between different nodes, a necessary condition to insure the continuity of the angular flux across the interfaces.

Figure V-23 shows the eigenvalue convergence of the  $P_3$  approximation versus the number of iterations. The eigenvalue oscillates at low iteration numbers but converges as the number of iterations

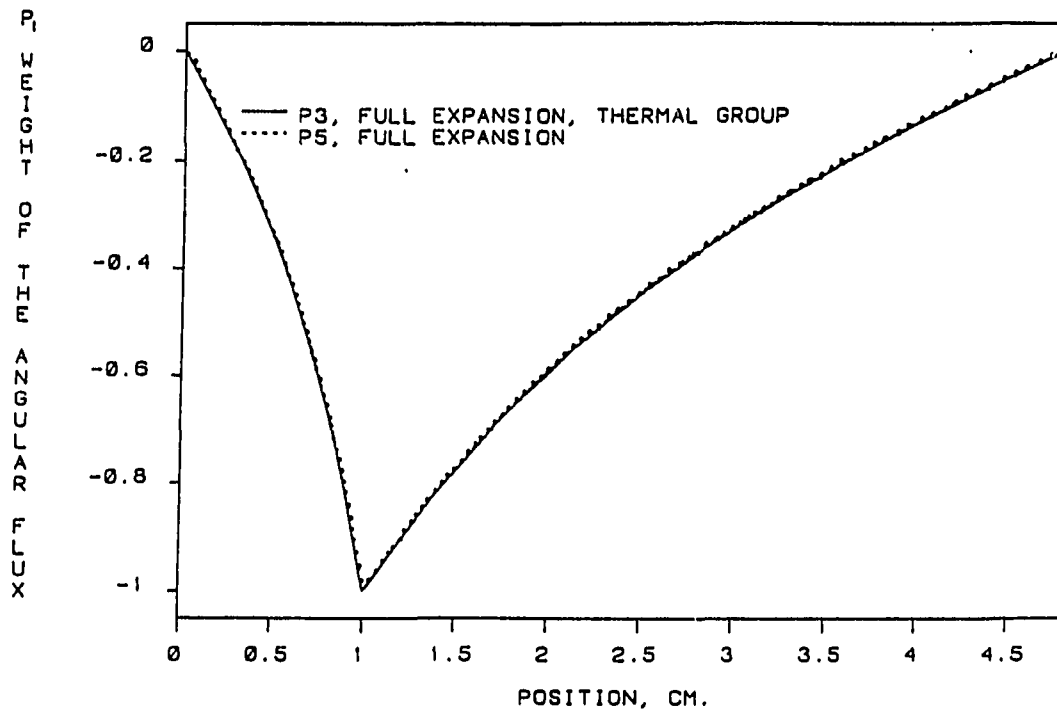


Figure V-18.  $P_1$  weight of the thermal flux for sample problem two

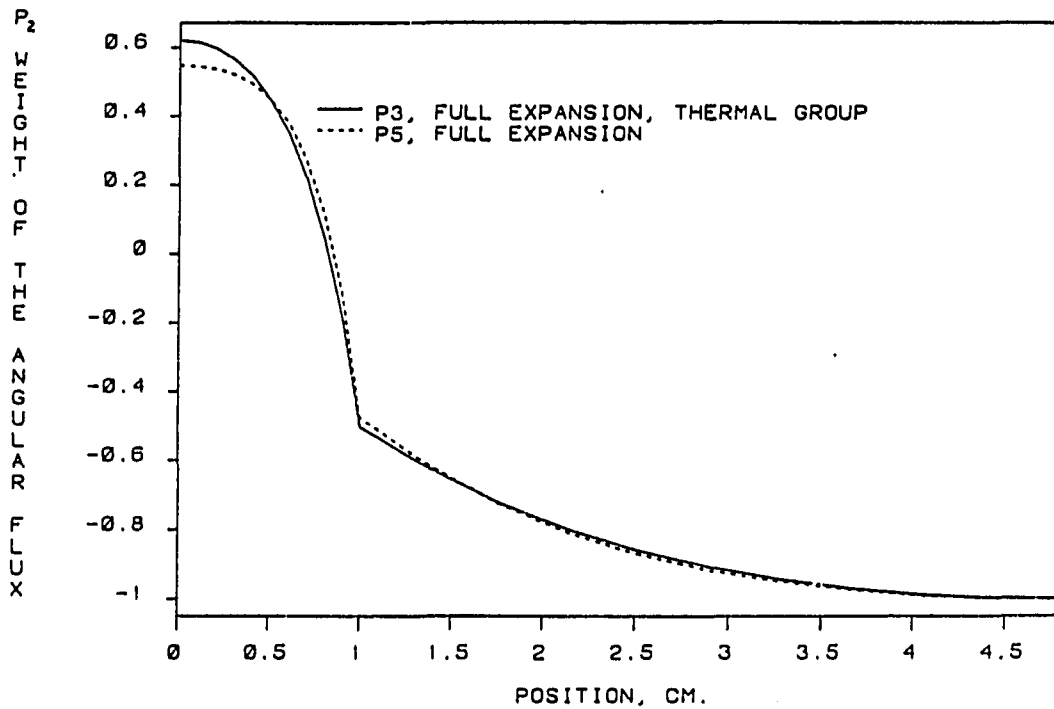


Figure V-19.  $P_2$  weight of the thermal flux for sample problem two

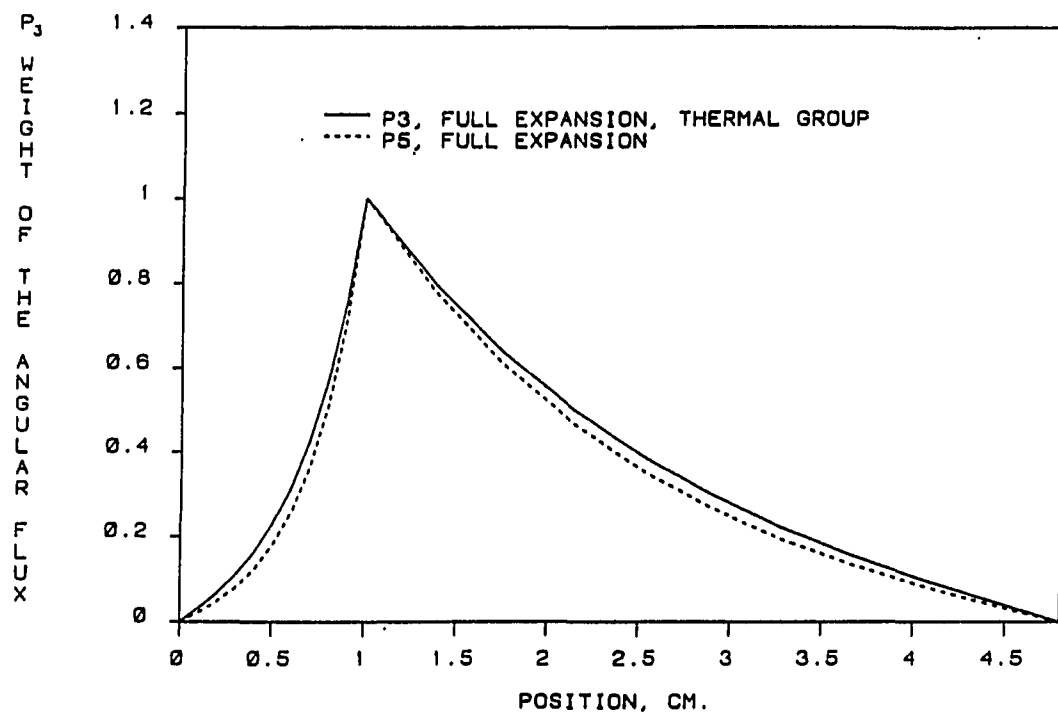


Figure V-20.  $P_3$  weight of the thermal flux for sample problem two

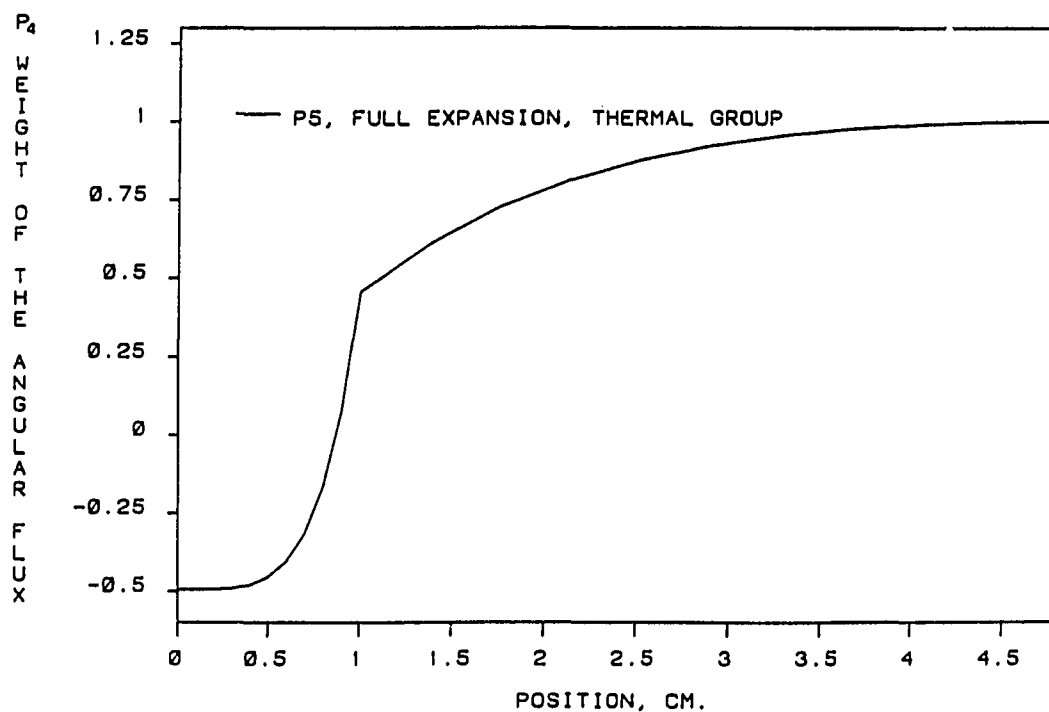


Figure V-21.  $P_4$  weight of the thermal flux for sample problem two

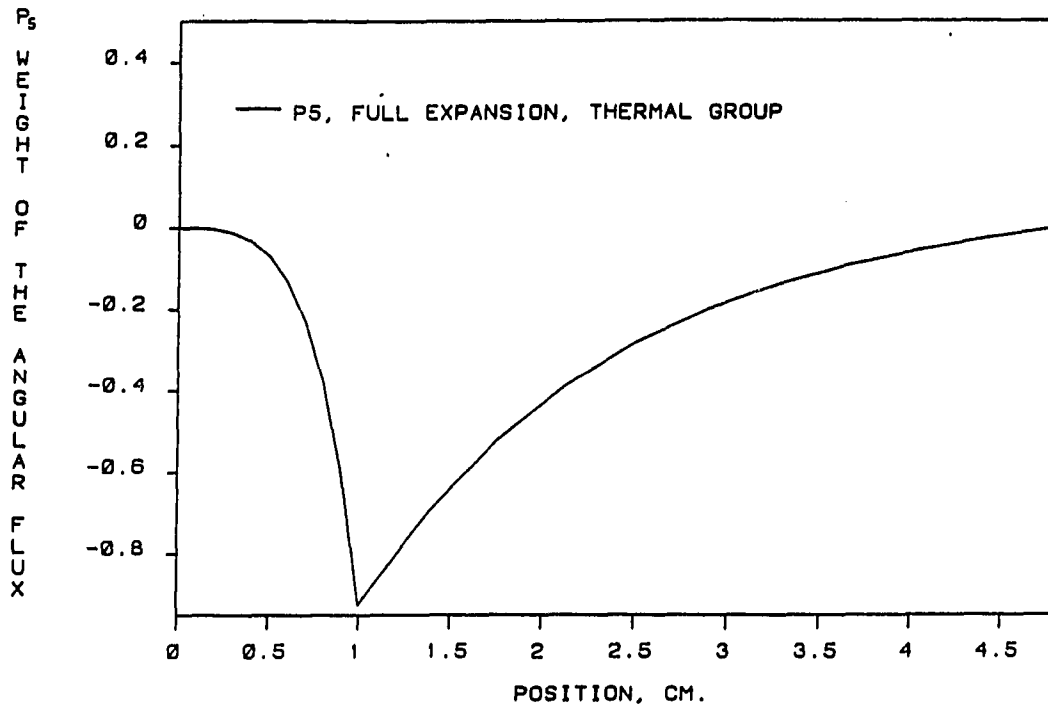


Figure V-22.  $P_5$  weight of the thermal flux for sample problem two

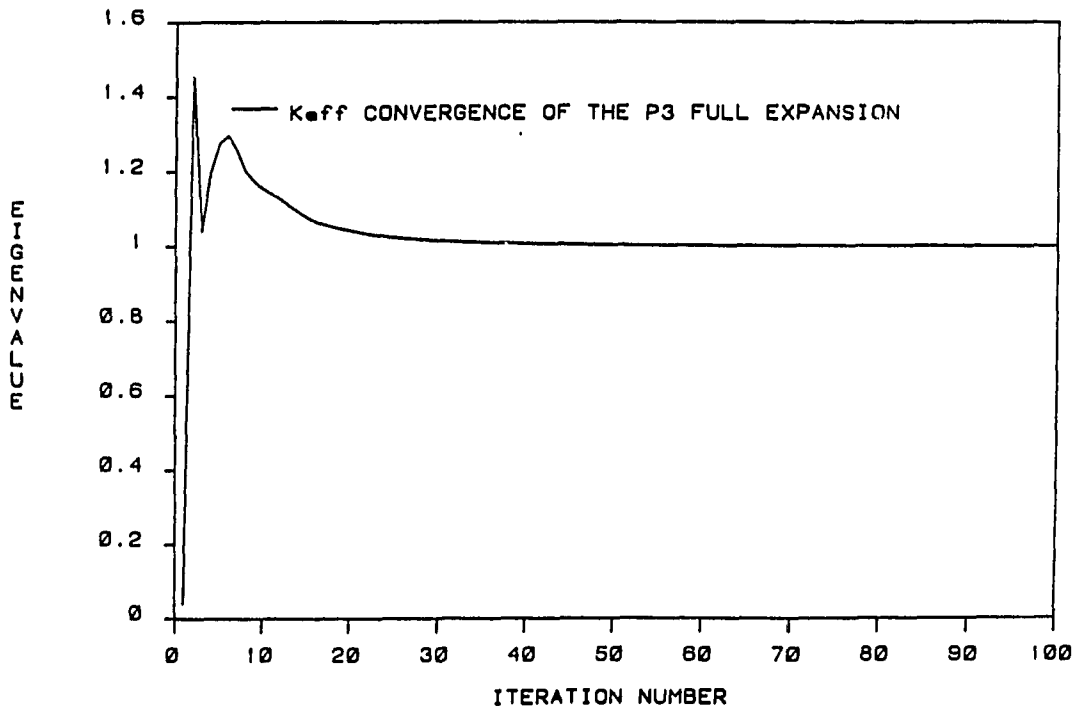


Figure V-23. Eigenvalue convergence of sample problem two

increases.

The sample problem presented here illustrates the capability of the TONODE code in determining the angular dependency of the neutron flux. The least squares minimization and the continuity of the angular neutron flux across the internal interfaces proved to be accurate even though only the odd moments of the neutron flux were required to be continuous in deriving the interface conditions. In this sample problem, only the full expansion was used since it was observed in the first sample problem that the partial expansion would not be capable of predicting an accurate solution where higher order  $P_N$  approximations are used.

## VI. SUMMARY AND CONCLUSIONS

The purpose of this study was to develop a one-dimensional nodal model that could be used in approximating a solution to the multigroup form of the neutron transport equation. The  $P_N$  approximation of the spherical harmonics method was used as the starting point in the development of the model. The expansion coefficients of the  $P_N$  equations were expanded in a series of Legendre polynomials. Two sets of Legendre polynomial expansions were used, which were arbitrarily called full and partial expansions. In the full expansion, the order of the spatial polynomial remains the same with increasing orders of angular dependency. However, in the partial expansion the order of the spatial polynomial decreased with increasing orders of angular dependency.

Since the polynomial expansions are not the exact solutions, residuals were obtained from the  $P_N$  equations. The residuals were then minimized by using the least squares technique of the finite element method. In doing so, relatively simple relationships were obtained for the unknown polynomial coefficients. However, these relationships were not sufficient to determine the unknown coefficients which, in turn, required the use of the interface conditions. The odd moments of the angular neutron flux over the half ranges were required to be continuous at the internal interfaces, and the Marshak boundary condition was used at the external boundaries. Using the interface and boundary conditions, enough relationships were obtained to solve for the unknown coefficients. The calculated polynomial coefficients

were then used to evaluate the effective multiplication factor; and new interface fluxes. An iterative process was applied and continued until a converged solution was obtained.

Two sample problems were developed to test the nodal model for accuracy of solution. The first sample problem included a comparison of the  $P_1$  approximation to a fine mesh finite difference solution to the neutron diffusion equation. The second sample problem included a comparison of the  $P_N$  approximation to the results of a discrete ordinates numerical solution of the transport equation. The polynomial expansion used a fourth order polynomial expansion for the spatial variable.

From the results of the first sample problem, it was concluded that the partial expansion of the model should only be used for development of low order  $P_N$  approximations. This is due to the fact that the least squares technique has trouble minimizing the difference between the second-order derivative and the remaining fourth-order polynomial terms in some of the  $P_N$  equations. On the other hand, both sample problems illustrated the capability of the full expansion of the model to accurately predict the solutions of the  $P_N$  equations. However, it was observed that a fourth-order polynomial expansion of the model is probably not adequate in cases where severe flux gradients occur. In these cases, it may be necessary to increase the number of nodes, or use a higher order polynomial expansion to get a better match between the derivative term and the remaining terms in the  $P_N$  equations.

The one-dimensional nodal model is not significant for practical

use since the one-dimensional fine mesh discrete ordinates equations can easily be solved. However, certain properties of the model can be studied and explained in the simpler one-dimensional framework and then extended and tested in the more complicated two and three dimensions.

## VII. SUGGESTIONS FOR FUTURE RESEARCH

The following suggestions are made for possible future research:

1. A study should be performed for cases where severe flux gradients occur. The number of nodes used in the study should be changed in order to observe the effect on the results of the model. When this study is completed, a set of guidelines could be developed to predict the number of nodes that are necessary for different problems.
2. A computer code that uses a higher order polynomial expansion could be developed and tested for cases where large flux gradients occur. This task is facilitated since the relationships for determining the unknown polynomial coefficients have already been developed in this study.
3. Since an interative technique is used to find the unknown coefficients, the rate of convergence becomes important. Therefore, it may be necessary to use an accelerating method such as the relaxation technique to enhance the convergence of the system. A numerical technique should then be developed to successfully predict the input relaxation parameters. This is an important area since the convergence rate of the system could depend on these parameters.
4. Expressions analogous to those of the one-dimensional model can be developed for two- and three-dimensional models. If this is done, two- and three-dimensional calculations should be performed and compared with other transport equation solutions.

## VIII. REFERENCES

1. A. F. Henry. Nuclear Reactor Analysis. The MIT Press, Cambridge, Massachusetts, 1975.
2. H. W. Graves, Jr. Nuclear Fuel Management. John Wiley & Sons, New York, New York, 1979.
3. G. I. Bell and S. Glasstone. Nuclear Reactor Theory. Van Nostrand Reinhold Company, New York, New York, 1970.
4. M. Feiz. Application of Finite Element Nodal Model to Multigroup Diffusion Theory. Unpublished M.S. Thesis, Iowa State University, Ames, Iowa, 1983.
5. A. F. Rohach. A Polynomial Nodal Model Using Legendre Expansion. *Annals of Nuclear Energy*, 13, No. 2:12-34, 1986.
6. J. J. Duderstadt and L. J. Hamilton. Nuclear Reactor Analysis. John Wiley & Sons, New York, New York, 1976.
7. K. Ganguly and A. Sengupta. A Transport Theoretic  $P_N$  Approximation. *Nuclear Science and Engineering*, 74:1-12, 1980.
8. R. J. J. Stammier and M. J. Abbate. Methods of Steady-State Reactor Analysis in Nuclear Design. Academic Press, New York, New York, 1984.
9. R. T. Ackroyd. A Finite Element Method for Neutron Transport. I. Some Theoretical Considerations. *Annals of Nuclear Energy*, 5, No. 2:75-94, 1978.
10. R. T. Ackroyd. The Why and How of Finite Elements. *Annals of Nuclear Energy*, 8, No. 11/12:539-566, 1981.
11. C. S. Desai. Elementary Finite Element Method. Prentice-Hall, Inc., Englewood Cliffs, N.J., 1979.
12. F. Schmidt and R. Fremd. Experience in Using the Finite Element Method for Reactor Calculations. *Annals of Nuclear Energy*, 8, No. 11/12:567-580, 1981.
13. M. K. Jain. Numerical Solution of Differential Equations. Halsted Press, New York, New York, 1985.

14. M. R. Wagner and K. Koebke. Progress in Nodal Reactor Analysis. Atomkernenergie, Kerntechnik, 43, No. 2:117-125, 1983.
15. H. W. Graves. Evaluation of Coupling Coefficients in Nodal/Modal Analysis. Annals of Nuclear Energy, 11, No. 5:213-223, 1984.
16. J. Askew. Summary of The Meeting; Calculation of 3-Dimensional Rating Distributions in Operating Reactors. Organization for Economic Cooperation and Development, Paris, 1979.
17. M. R. Wagner. Current Trends in Multidimensional Static Reactor Calculations. Proceedings of The Conference on Computational Methods in Nuclear Engineering, April 1975.
18. E. T. Whittaker and G. N. Watson. Modern Analysis. Cambridge University Press, London and New York, 1940.
19. M. Feiz. TONODE Code. Department of Nuclear Engineering, Iowa State University, Ames, Iowa, 1986.
20. Numerical Determination of the Space, Time, Angle, or Energy Distribution of Particles in an Assembly. Argonne Code: Benchmark Problem Book. Supplement 2. Argonne National Laboratory, Oak Ridge, Tennessee, June 1977.
21. A. F. Rohach. TODMG Code. Department of Nuclear Engineering, Iowa State University, Ames, Iowa, 1986.

## IX. ACKNOWLEDGMENTS

The author is indebted to his major professor, Dr. Alfred F. Rohach, for his support, interest, suggestions, and encouragement during the various phases of this research. In addition, the author wishes to express his special appreciation to the Department of Nuclear Engineering for a departmental assistantship. Special thanks go to Dr. Bernard I. Spinrad, Dr. Richard A. Donofsky, Dr. Donald M. Roberts, Dr. Thomas R. Rogge, Dr. Rajbir S. Dahiya, Mr. Mohammad Benghanam, Mr. Jordi Roglans, and Mr. John Sankoorikal for their many helpful suggestions and discussions during the time this study was performed.

Finally, the author wishes to thank his parents, Mr. and Mrs. Reza Feiz, and his brothers Saied, Hamid, and Vahid Feiz. The author wishes to acknowledge his first teacher, Mr. Hassan Komaylie.

## X. APPENDIX

The Legendre polynomials are defined by the following relations:

$$P_0(x) = 1 \quad (X-1)$$

$$P_n(x) = \frac{1}{2^n n!} \frac{d^n}{dx^n} (x^2-1)^n \quad n=1,2,\dots \quad (X-2)$$

The first few polynomials are:

$$P_1(x) = x \quad (X-3)$$

$$P_2(x) = \frac{1}{2} (3x^2-1) \quad (X-4)$$

$$P_3(x) = \frac{1}{2} (5x^3-3x) \quad (X-5)$$

The Legendre polynomials satisfy the following recurrence relation for  $n \geq 1$ .

$$(2n+1) x P_n(x) = (n+1) P_{n+1}(x) + n P_{n-1}(x) \quad (X-6)$$

The derivative of the Legendre polynomials could be obtained by the following relationship for  $n \geq 1$ :

$$\frac{dP_n}{dx} = \sum_{i=1}^n (2i-1) P_{i-1}(x) \quad (X-7)$$

if  $n$  is odd,  $i$  takes only odd values

if  $n$  is even,  $i$  takes only even values

The Legendre polynomials form a complete set of orthogonal

functions on the interval  $-1 \leq x \leq +1$ . They satisfy the orthogonality relation

$$\int_{-1}^{+1} P_m(x) P_n(x) \frac{dx}{2} = \frac{\delta_{mn}}{2n+1} \quad (\text{X-8})$$

where  $\delta_{mn}$ , the Kronecker delta, is unity if  $m=n$  and zero otherwise.